ACC target performance setting via NDS big data analysis

E. Pizzigoni

TU Delft

ACC target performance setting via NDS big data analysis

by

E. Pizzigoni

in partial fulfillment of the Master of Science degree
in **Mechanical Engineering** - Vehicle Engineering
at the Delft University of Technology,
to be defended publicly on Tuesday July 2, 2019 at 09:00 AM.

Student number:	4631919	
Project duration:	July 24, 2019 – July 2, 2019	
Thesis committee:	Prof. dr. ir. R. Happee,	TU Delft, supervisor
	Dr. ir. M. Wang,	TU Delft
	Ir. J.C.J. Stapel,	TU Delft

TU Delft TOYOTA

Abstract

Advanced Driving Assistance Systems (ADAS) technologies like Adaptive Cruise Control (ACC) are becoming the normality for many users, and many major car manufacturers are introducing SAE level 2 and 3 [1] automation systems [2–4] into the market. The main advantage of Automated Vehicles (AV) will be the significant decrease in road accidents and casualties [5, 6]. However, a significant shift from conventional to automated vehicles must occur before it can have a positive impact on society. If the behaviour of the vehicle is not perceived as natural, the user will most likely not activate the ADAS features again. During this study a naturalistic dataset is used to investigate the driver behaviour, in the hope of bringing the current ACC logic to a more human-like behaviour that will feel more natural to the driver.

The research question summarizes the final objective of this study: *How can Naturalistic Driving Study (NDS) datasets be used in target performance setting for ACC systems?* In particular, this study will answer the research question by studying human behaviour in the scene of *following an accelerating vehicle*. The main body of this thesis is divided in three chapters, one for each step of the research. First, in Chapter 2, the information about the used datasets are provided together with the methodologies used to extract the relevant time-series data. Secondly, in Chapter 3, driver behaviour models are created in order to mathematically characterize human behaviour. The strength of the created models is their ability to represent the full range of driver behaviour in terms of driving style. The *aggressiveness* parameter of the model can be easily adjusted to represent different percentiles of driver behaviour. This allows for a quick and effective tuning process: by changing a single parameter the driving style of the model can be fully modified. Finally, in Chapter 4 the driver behaviour models are implemented into a simulation environment. The models are simulated against an existing ACC logic in order to assess the difference in behaviour. The comparison highlighted two conclusions: first, the ACC logic behaves in a very conservative way compared to driver behaviour, especially when starting from standstill. Secondly, the *aggressiveness* kept by the ACC logic was not consistent throughout the speed range. This variation of the logic's driving style could result even more bothersome to the customer than its general conservative behaviour. The string stability of the driver behaviour models was also assessed. Although the proposed logic proved more stable than the regular ACC logic, it still cannot reach full string stability.

Hopefully, with the method developed in this study, the process of getting accustomed to this new technology will become easier for the customer. Thanks to the driver behaviour models the motion of the vehicle can feel familiar and predictable, with the controller becoming part of the Human Machine Interface (HMI). As the customer gets more familiar with this technology his expectation will also increase and change, especially as the levels of automation start to increase. This will inevitably push automakers to continue to improve the technology to deliver increasingly advanced and safe vehicles.

Keywords: *ACC, ADAS, driver behaviour, automated vehicle, naturalistic driving study, driver model, car-following*

Definitions

Table 1: List of acronyms.

ACC	Adaptive Cruise Control
ADAS	Advanced Driving Assistance Systems
AEB	Automated Emergency Braking
AP	Acceleration Percentile
AV	Autonomous Vehicles
CACC	Cooperative Adaptive Cruise Control
CC	Cruise Control
CFD	Cumulative Distribution Function
DP	Distance Percentile
ECU	Electronic Control Unit
FCW	Forward Collision Warning
FOT	Field Operational Test
GEV	Generalized Extreme Value
GM	General Motors
HMI	Human Machine Interface
IDM	Intelligent Driver Model
KPI	Key Performance Indicator
LDW	Lane Departure Warning
NDS	Naturalistic Driving Study
RMSE	Root Mean Square Error
SiLS	Software in the Loop Simulation
THW	Time Headway
UA	User Acceptance
VMC	Vehicle Management Centre
WTP	Willingness To Pay

Nomenclature

τ	Driver reaction time delay [s]
a_e	Ego vehicle acceleration [m/s^2]
a_t	Target vehicle acceleration [m/s^2]
D_r	Relative distance (or headway) between ego and lead vehicle [m]
h_0	Desired following distance at standstill [m]
h_d	Desired following distance [m]
h_v	Constant THW contribution to h_d [s]
j_e	Ego vehicle jerk [m/s^3]
V_e	Ego vehicle speed [m/s]
V_r	Relative speed between ego and lead vehicle (negative when approaching) [m/s]

List of Figures

List of Tables

Contents

1 Introduction

With Advanced Driving Assistance Systems (ADAS) already being standard equipment for the majority of new vehicles, automated driving is the biggest change happening to the transportation industry since the replacement of horse carriages. ADAS technologies like Adaptive Cruise Control (ACC) are becoming the normality for many users, and many major car manufacturers are introducing into the market SAE level 2 and 3 [1] automation systems [2–4].

The main advantage of Automated Vehicles (AV) will be the significant decrease in road accidents and casualties [5, 6]. Despite this, a significant shift from conventional to automated vehicles must occur before it can have a positive impact on society. This evolution will be heavily influenced by the Willingness to Pay (WTP) and by the faith that customers will have in the technology. Bansal and Kockelman [8] tried to forecast the long-term adoption of AV's by the American citizens. They estimated that by 2045 the market penetration of AV's can be as low as 24.8% and as high as 87.2%. This high variance in the results is caused by the different levels of WTP, highlighting the importance of the human factor in the design of these types of technologies. If the client does not see the technology as an added value to his/her driving experience the WTP will not be high enough to allow a quick market penetration of these technologies.

1.1. Research Question

If the design process of automated devices is only based on how good the technology works, there is a high risk that the customers will not respond to the product as expected: the User Acceptance (UA) of the customer might be low due to trust issues towards the automation. The Psychology department of the University of Toronto tried to understand trust between humans and the automated system [9]. It was found that trust was built with experience, in a very similar way to how trust between human beings increases. The task of the engineer is to accelerate this process via a user-friendly experience. For instance, in the design of ADAS systems, the support provided by the automated system should be perceived as natural. If a Front Collision Warning (FCW) system has a very early trigger compared to the normal breaking behaviour of the driver, the system will be likely switched off by the user, thus also losing acceptance in more advanced systems like Automated Emergency Braking (AEB). To cope with this issue from the early stages of the design process, Toyota Motor Europe is undertaking a series of research activities focused to study naturalistic driving behaviour using "big data". These studies will be used to set humanlike target performance for ADAS systems.

The following research will be focused on target performance setting for the ACC system, focusing on scenarios where the driver is accelerating when following a leading vehicle. The user feedback regarding the current system shows that acceleration levels are very conservative, especially

at low speeds. Studying a 580,000 km database recorded in the EuroFOT project, the objective is to model driver behaviour and investigate how it differs from current logic's. Subsequently, it will be possible to consider how the control logic of the ACC can be modified to achieve a more naturalistic response. In performing this type of research it is important to keep into consideration the fact that people often do not want to be driven in the same manner as they drive. The perception of driving style as a passenger is different from a driver's [10]. For this reason, throughout the whole research it will be crucial to keep in mind the human factors involved. The main focus of the project can be summarized in the following research question:

How can Naturalistic Driving Study (NDS) datasets be used in target performance setting for ACC systems?

The main challenges of this study are formulated in the following sub research questions:

- *How can the variance of driver behaviour be modelled?*
- *What driving styles are more suitable for the comfort of the driver?*
- *What are the shortcomings of current ACC logic?*
- *How can the logic be improved in accelerating car-following scenarios?*

1.2. Literature Review Conclusions

Before starting this project a literature review was conducted and the conclusions gathered are summarized below, more information can be found in the literature review report. The existing research studied can be divided into two main categories. The first part is focused on previous attempts in driver behaviour modelling and on the possibly useful information to the modelling process, like human perception. The second part covers all the human factor aspects related to the ACC system.

- *Driver Modelling:* since driver behaviour models use vehicle states as inputs it is important to understand how humans perceive these states, thus human perception was analysed. From literature it seems that the human eye perceives driving speed using optic flow [11, 12]. For approaching emergency situations research has shown that drivers use looming to get the information relative to the lead vehicle [13–15]. This means that drivers are directly able to infer the relative states. In steady state *following* situations, research has shown that drivers tend to keep a constant Time Headway (THW) at every driving speed [16–18], this information is very useful for the design of the ACC logic. Driver modelling for traffic simulation purposes was found to be a very broad field. The attention was focused on two types of models: continuous [19–22] and psychophysical [23–26]. The strength of the continuous models is their ability in correctly approximating the general behaviour of the driver, unfortunately, they are not accurate enough to give detailed acceleration estimates. They also are not able to represent different driving manners apart from the one used to fit them. Psychophysical models offer a different approach on the car-following problem: their intent is to integrate human biological limitations in the modelling process. This is achieved through the use of perceptual thresholds. Overall it is hard to judge the accuracy of the psychophysical models since the implementation of the thresholds is often done in a very peculiar manner. The biological meaning of the thresholds also poses some difficulties in the calibration process of these types of models. The coherence deriving from the biological meaning of the perceptual thresholds is the main advantage of these models. Many implementations of the psychophysical models are, by definition, discontinuous and this could create discomfort in the driver.

- *ACC Human Factors:* the human factors involved in this type of device are crucial to understanding the difference between the driver and the passenger perspective. Even if this information is not directly used in the modelling process, how humans approach this technology should always be kept into consideration during the design process. It has been seen from numerous studies in literature that the ACC has both positive and negative impacts on the driver. The use of an ACC tends to lower the average driving speed and helps to comply with the speed limits [27, 28], on the other hand, it worsens the reaction time to potentially dangerous situations in which the user needs to take back full control of the vehicle [29, 30]. From a comfort perspective, optimal controller tuning should be achieved to enable smooth longitudinal and trajectory automation, moreover the car needs to keep a behaviour which is perceived as safe by the user. Motion sickness is already quite a common issue which is further aggravated by automated systems, the lack of control has been shown to be the principal cause to increase car-sickness [31, 32]. A thoughtful design of the HMI can aid mitigate the issue: the screens should have a moderate size and be positioned at the height of the horizon [33, 34]. Trust and user acceptance are important aspects in defining the adoption rate of the new technology. Many research examples already looked into users' trust in automated systems [9, 29, 35–37]. The common conclusion of almost all the papers found is that the negative effects of the system, both in terms of trust and driver behaviour, are diminished with experience if the user is correctly informed about the functionality and the limitations of the automated system. This highlights a very important aspect of the design of ADAS features.

Few gaps in current research were observed during the literature review. No driver model was found that was able to specify different driving styles. The ability to choose a certain driving manner without the need of recreating the model would give a great advantage during the tuning of the controller. It was also noticed that no previous research found used extensive NDS dataset to create such driver model. The only example was from Moon and Yi [38], although it represents an interesting example the methodology still has many limitations. The focus of the master thesis project will be to try to cover these research gaps and to understand the impact of this study on the design of an ACC system.

1.3. Method Overview

In order to achieve the objectives set in the research question it is necessary to develop a proper methodology. Figure 1.1 shows a diagram explaining the process followed in this study.
The first step is to collect the data. The dataset used in this study is the result of a European funded project called EuroFOT. During this project 35 participants drove their own vehicle for approximately one year. This resulted in a total of 581.347 *km* and 13.407 hours of naturalistic driving data. More details about the data will be covered in Section 2.1.

From the continuous recordings of the driving data it is necessary to extract the driving scene of interest. In the example of this thesis the scene studied is *following an accelerating vehicle*. Other examples can be: driving in corners or braking when approaching another vehicle. Given the extensive size of the dataset this process cannot be done manually, hence an algorithm needs to be programmed in order to extract the driving scenes automatically. The algorithm needs to be thoroughly designed and validated. If the detection includes unintended samples this will created biases in the statistical analysis. The detection logic will be treated in detail in Section 2.2.

Once the driving scene is extracted it is possible to analyze the data and develop the driving behaviour model. The driver behaviour models developed in this study take into consideration three aspects: the driving conditions, the driving behaviour and the driving manner. The driving conditions are all the factors that define the context to the scene that will ultimately influence the driving behaviour. Finally the driving manner (or style) is assumed to be the variation in driving behaviour that is not caused by the driving conditions. Modelling the driving manner allows more

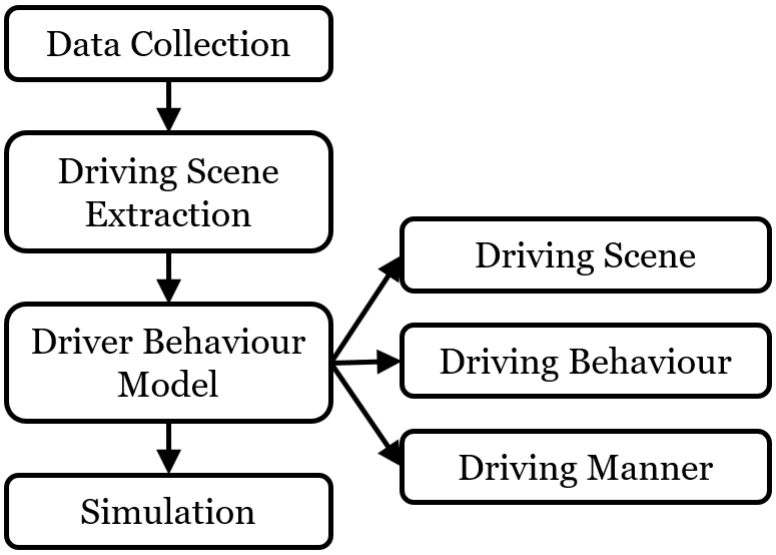

Figure 1.1: Methodology overview.

aggressive and calmer behaviours from the same or different drivers to be included in the model. This gives great advantages during the implementation process as it's easily possible to adapt the driving style to the system to what the most suitable driving manner is. The driver modeling portion of this project will be covered in Chapter 3.

The final step of this study is to convert the driver model into a simulation environment. The fact that a behaviour model represents well the drivers intentions does not necessarily make it useful. A model needs to be implementable, both in a simulation environment and directly in a real vehicle. During this process a set of challenges can arise, from the fact that the model needs to run online to the robustness to real life sensor accuracy. The simulations performed in this project have the aim of comparing the current ACC logic with the proposed changes coming from the NDS study. Details about the simulations will be covered in Chapter 4.

1.3.1. Following an Accelerating Vehicle

The methodology explained above can be applied to different driving scenes. In this project the analysis will be focused on the *following an accelerating vehicle scenario*. In this scenario, the lead vehicle (also referred to as the target vehicle) accelerates whilst remaining in the same lane, and as a reaction the ego vehicle (the instrumented one) follows the acceleration whilst also still remaining in the same lane. Only the events with a reaction of the ego vehicle are considered in this study. As is shown in Figure 1.2, this event is considered to happen whilst the ego vehicle follows the lead vehicle. In Figure 1.2 it is also possible to see that after the acceleration event the driver will either reach his desired speed or will go back to the *following* state. The context of the scene and its relationship with the *following* behaviour will cover an important role in this project as will be explained in the next chapters.

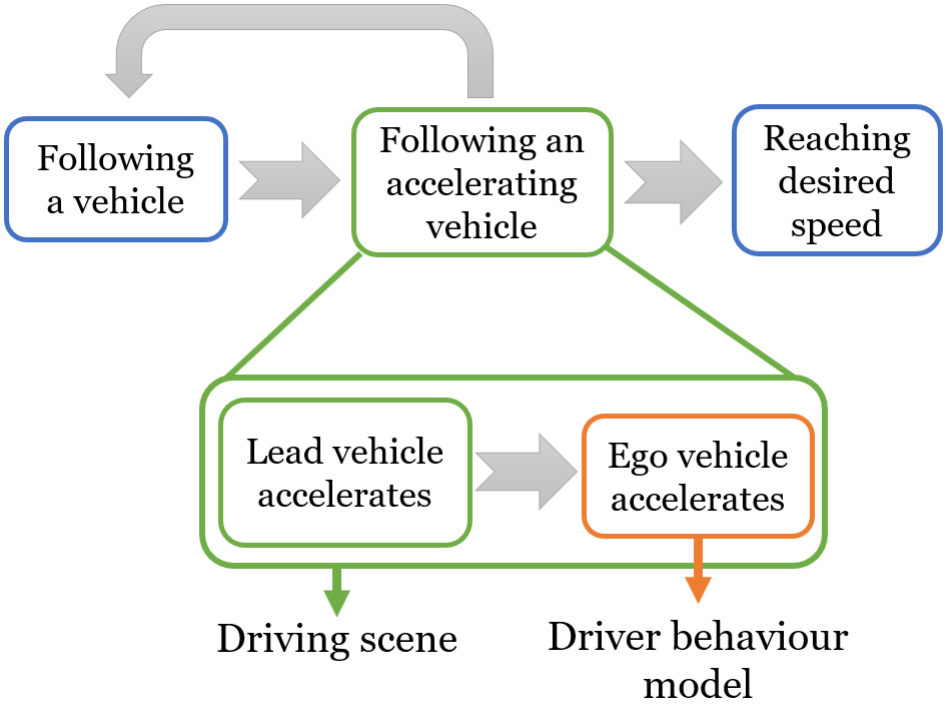

Figure 1.2: Driving scene overview.

2

Data Extraction

This chapter will cover the scenario extraction process. More information about the data used will also be treated. One of the challenges of working with large amounts of data is to be able to filter the information which is not considered relevant in the scope of the study. In the case of this project it was necessary to extract the *following an accelerating vehicle* scenario from the hours of continuous driving. The process and the algorithms used are explained in the chapter.

2.1. EuroFOT Data set

Started in May 2008, the EuroFOT project is one of the biggest Field Operational Tests (FOT) ever performed in Europe. Overall the project was financed with 21.6 million Euros, 65% of which was provided by the European Commission [39]. Some of the biggest automakers together with the suppliers of ADAS systems like Bosch and Continental also joined the project as partners [7]. The main objective of the project was the evaluation of the impact of ADAS systems, like ACC and LDW, both from a technical and a socio-economic point of view. Different systems were studied in the 4 different Vehicle Management Centers (VMC's) across Europe. An overview of the different VMC's constituing the EuroFOT project is shown in Figure 2.1.

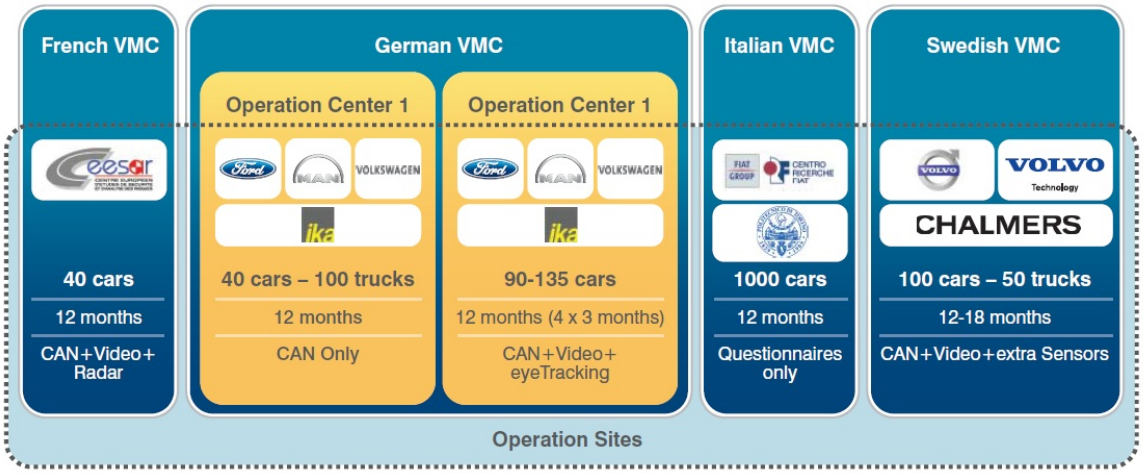

Figure 2.1: Vehicle Management Centers (VMC's) constituting the EuroFOT project [7]

The data used and analyzed in this study was only the one gathered and provided by CEESAR in the French VMC. It was only possible to use the French data set because it is the only one which

includes a radar sensor in the vehicles, providing the estimated distance and relative speed of the lead vehicle. The data logging has been done over the period between 2010 and 2012 with a total of 40 vehicles driven by non professional drivers. The vehicles used were 21 Renault Laguna 3 and 14 Renault Clio 3 with manual transmission, these 35 vehicles were driven by ordinary drivers whilst the remaining 5 were driven by CEESAR employees. Due to cost and privacy reasons the equipment of the two groups of cars was different, an overview of the instruments used on both vehicle groups is shown in Table 2.1. The first group of vehicles drove for approximately one year, while the CEESAR group drove for 6 weeks spread across the two years testing period. An overview of the length and duration of the data gathered can be found in Figures 2.2a and 2.2b, a total of 581.347 km was recorded during 13.407 hours of driving.

Table 2.1: Equipment of test cars used in French EuroFOT.

Equipment	**35 Ordinary Drivers**	**5 CEESAR Drivers**
CTAG Datalogger 2	YES	YES
GPS	YES	YES
Data Transfer Method	GPRS	Manual
TRW AC20 Radar	YES	YES
Custom VideoLogger (H.264)	NO	YES
Cameras	0	4
Mobileye AWS	NO	YES
Smarteye Eyetracker	NO	YES

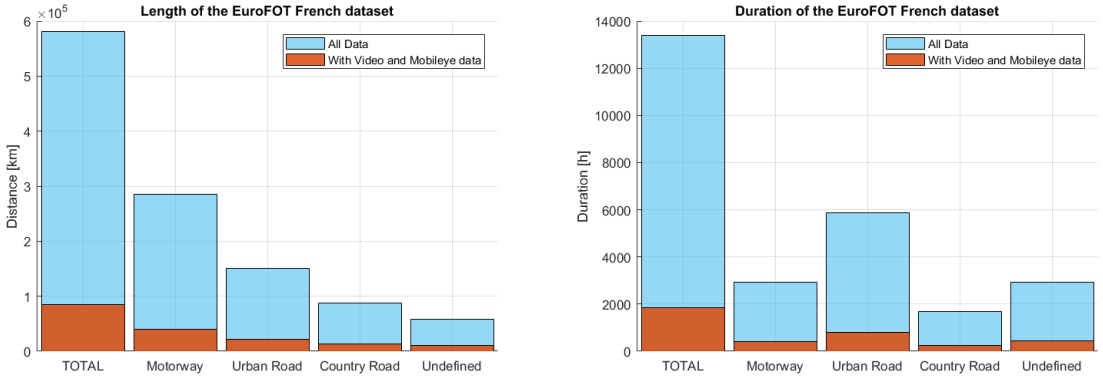

(a) Length overview of the EuroFOT French data set. (b) Duration overview of the EuroFOT French data set.

Figure 2.2: Overview of length and duration of the EuroFOT data set

2.2. Scenario Extraction

The selection of a consistent extraction algorithm is a crucial step when analyzing big FOT data sets. The extraction process limits the available data for the analysis. This means that there is a risk of excluding important or interesting episodes, hence creating biases in the final data set. The added difficulty in the design of these kinds of algorithms is that often there is no absolutely correct answer. Often it is necessary to find a balance between the amount of data and its quality. If the detection conditions are very strict the scenarios detected will be more consistent, with the downside being that many cases potentially containing relevant driving patters may be discarded.

During the development of the algorithm the effect of every change in the logic was always monitored by visually checking the result. The main focus was to make sure that all the detected scenar-

ios were clearly pertinent to the study. In some cases, even if a particular scenario was satisfying the conditions it was impossible to detect, even visually, the most basic KPI's. For this reason, only the cases which were clearly acceleration scenarios were included in the extraction. To guarantee consistency within the extractions, if the scenario did not comply with the requirements it was discarded. Previous versions of the algorithm were structured in such a way that if a detection method failed then an alternative one was used. It was soon clear that this created an inconsistency within the different scenarios as it is challenging to create an alternative detection logic which produces a similar outcome. The method used in this study is now explained. Starting from a continuous time series record, this method will produce the singular segments with the acceleration episode.

2.2.1. Start Timing Detection

The most important part of the acceleration episodes is the beginning. In particular both the target and ego vehicle start timing. The start timing is defined as the exact moment in which the target and ego vehicle start the detected acceleration episode. The procedure developed to robustly detect the start timing point is shown below:

1. Search every point after the lead vehicle speed increases more than $7.5 km/h$ in a 4 seconds time window. Approximately equivalent to a $0.5 m/s^2$ average acceleration.

2. The same speed increase condition is applied to the ego vehicle.

3. For each point detected in the previous two steps the corresponding point was found in which the speed is $6.5 km/h$ less than the speed that triggered the previous conditions. This will result in a first estimate of the start timing.

4. All possible end points are detected. An end point is found whenever the ego speed increase is less than 0 for 2 consecutive seconds.

5. Every target start timing is associated with ego start and end. If one of the three is missing all the episode is discarded. A new episode should not start if the previous is not ended.

6. Finally the corrected start timing is calculated. Using a threshold on the jerk, the bend point in the speed is found in a time window of two seconds before the estimated start timing. Since the precision of the start timing point is crucial in the study of this scenario, if the corrected point is not found the whole scenario is discarded.

Two examples of the detection logic can be seen in Figure 2.3 and 2.4. The first shows an example at standstill starting conditions while the second one, a case at higher speed. By comparing these two cases it is clear that precisely detecting the start timing point is easier in standstill cases as the acceleration start is more visible, creating an algorithm that worked at every starting speed was one of the the biggest challenges at this stage of the analysis.

In Figure 2.3 it's possible to see that the ego acceleration has an earlier onset than the speed. This is due to the filtering process executed by the supplier on the raw data. Since the acceleration signal is derived from the speed signal, the focus of the start timing detection was to get the bend-point in speed rather than the one in acceleration. In order to check the influence of the timing, the speed signal is compared with the integral of the acceleration and the acceleration to the derivative of the speed. The results are shown in Figure 2.5. Apart from some noise introduced by the derivative, the signals match correctly. To make sure that also the other signals are correct this check was performed on each measurement provided.

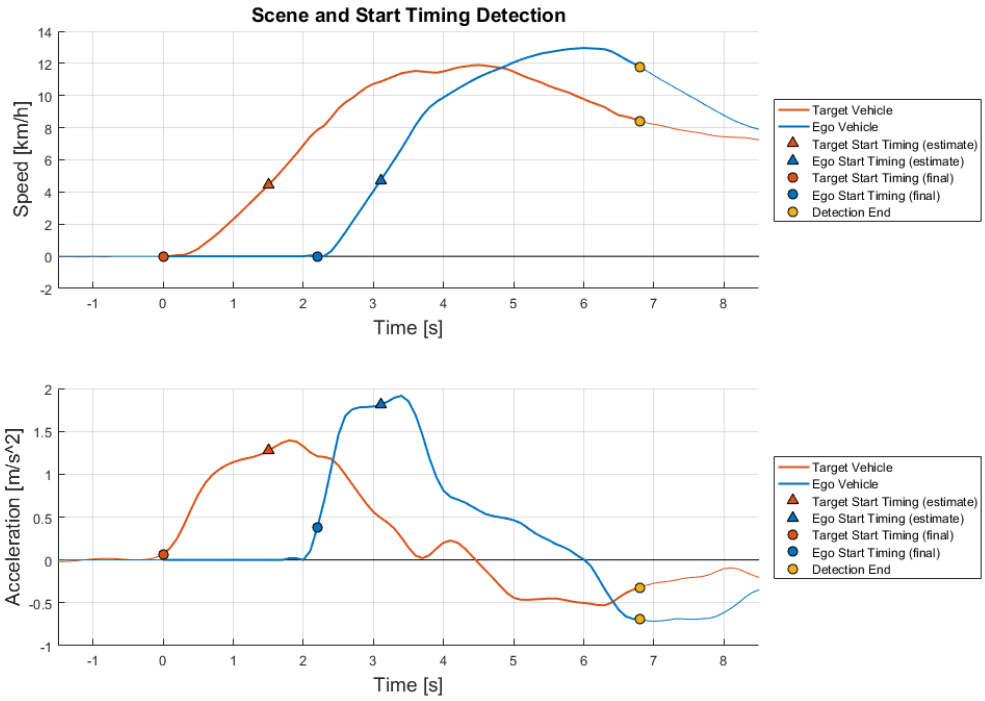

Figure 2.3: Example of scene extraction starting from standstill conditions.

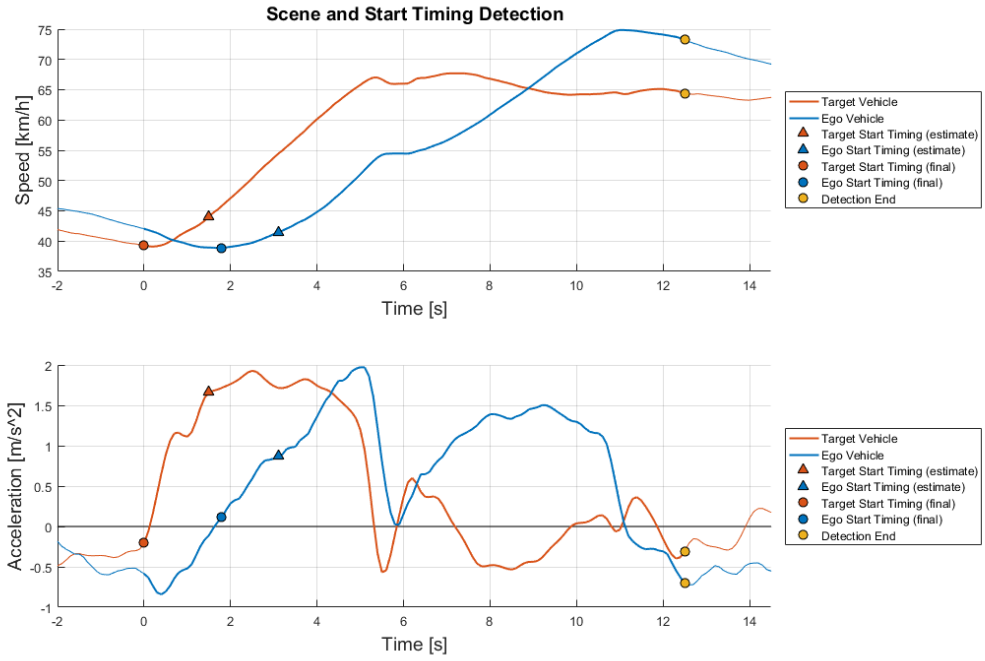

Figure 2.4: Example of scene extraction starting from middle speed conditions.

2.2.2. Additional Conditions

The fact that the start timings were found in an episode did not guarantee that the episode was interesting for the analysis, additional checks were needed to make sure that the episode detected was valid for the analysis. Firstly, it was necessary to check that the reaction of the ego vehicle was

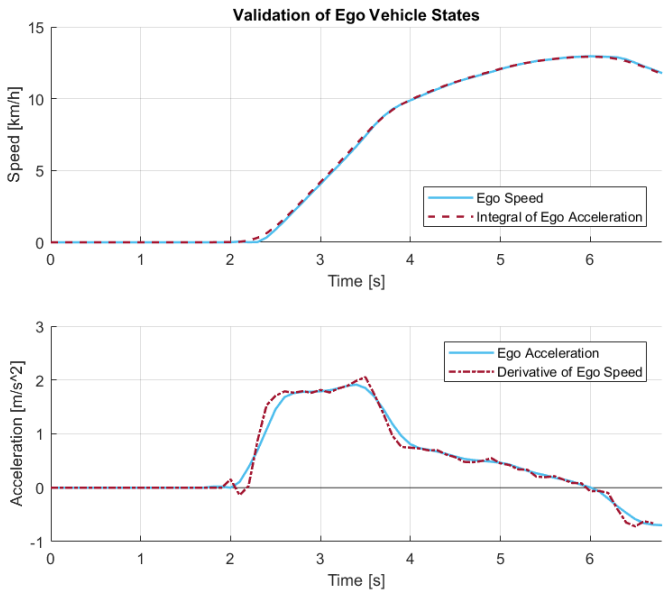

Figure 2.5: Validation of ego vehicle states.

caused by the target vehicle acceleration. This could not be inferred with absolute certainty but these conditions were set to increase confidence:

- Ego start timing must be after target start timing.
- Ego start timing must be within 5 seconds of the target start timing.
- The THW must be less than 2 seconds or the relative distance less than 10 meters at target start timing.
- The relative speed must be greater than $-5 km/h$ (negative when approaching) at target start timing. There is no upper limit for the relative speed.

Since the radar sensor can change or loose the target, additional checks were implemented together with the supplier to make sure that for the entirety of the detection the target did not change and was never lost. On top of that the target and ego vehicle need to drive in the same lane for the full duration of the episode.

2.2.3. Considerations about the detection logic

Finally, the extraction algorithm detected a total of 55.096 acceleration episodes. Via a visual validation the final version of the detection logic proved to be very robust and reliable. Other possible logics were also taken into consideration: the use of the throttle input sensor would have given the actual start timing as of the intention of the driver. Unfortunately, the throttle position sensor was often missing moreover the signal was in general more difficult to post-process due to its quality. By detecting the start timing with the acceleration, it was always possible to compute the throttle start timing afterwards in the cases where the signal was present.

2.3. Initial Acceleration Level Extraction

The conditions at start timing cannot give any information about the actual magnitude of the acceleration levels in the episode. For this reason the initial acceleration level is extracted from every

scenario, both for the ego and for the target vehicle. The aim was to get the acceleration value at the first bend point of the signal together with the corresponding jerk value. This value represents the first intention of the driver from an acceleration magnitude standpoint.

To be able to detect the most accurate point two different calculation methods are used and afterwards one of the two results is selected. The main method uses the jerk signal to detect the first bend point of the acceleration signal, this method is discussed more in detail in Section 2.3.1. The second method used is simply the maximum acceleration value in the episode. Once the two alternative acceleration values are determined, the corresponding mean jerk from the start to the selected point is calculated. Among the two methods, the one that yields the highest jerk value is selected as the final value, more about the selection method is reported in Section 2.3.2.

2.3.1. Bend Point Method

The aim of this calculation method is to find the first significant bend point in the acceleration signal. First the acceleration increase at every time instant is computed (2.1). Afterwards the condition in Equation 2.2 is evaluated, with $k = 0.15$.

$$\Delta a_i = a_i - a_{i-1} \tag{2.1}$$

$$a > 0 \quad \text{AND} \quad \Delta a > k \max(\Delta a) \tag{2.2}$$

The algorithm detects as the final point the first instance in which the condition becomes false for at least 0.4 seconds. The minimum duration criterion is needed to prevent that the condition is triggered by the small disturbances in the acceleration signal caused by the gear shift. This is one of the downsides of using vehicles with manual transmission. In only 240 cases the algorithm fails to find a point, these cases are very short episodes in which the acceleration always increases at the same rate, hence a bend point does not exist. In these cases the maximum value method is used as it still gives a representation of the acceleration level.

2.3.2. Acceleration Point Selection

If the bend point method found the relevant point then the selection between the two alternatives is done based on the corresponding jerk values. For both methods, the mean jerk value from the beginning to the detected point is computed. The method that yields the highest value in jerk is selected. This method was implemented because in uncertain conditions there is not always a clear correct point hence the bend point method struggles to detect the best one. An example of this issue is shown in Figure 2.6a.

In other cases it is possible for the incorrect point to be detected by the maximum value. If the acceleration signal has a clear bend point but afterwards keeps increasing, the maximum point will be very far from the beginning and it will not correctly represent the first intention of the driver. If the maximum point is too far from the beginning, its mean jerk value will be low hence the bend point will be selected. An example of this scenario is visible in Figure 2.6b.

2.3.3. Initial Acceleration Level Considerations

The detection of acceleration level was visually validated, and overall gives a reliable detection. In the great majority of the cases a clear bend point was easily detectable. As expected, not every driver always accelerates with a clear step acceleration and a clear bend point is often difficult to detect even manually. The algorithm was tuned to give a reference acceleration value also in these challenging cases. Overall the required precision of this algorithm is not as critical as the start timing as the position of the point is not as relevant. The algorithm reliably gives a good impression of the first acceleration intention of both the target and ego vehicle. This important KPI will later be used in the analysis of the driver behaviour.

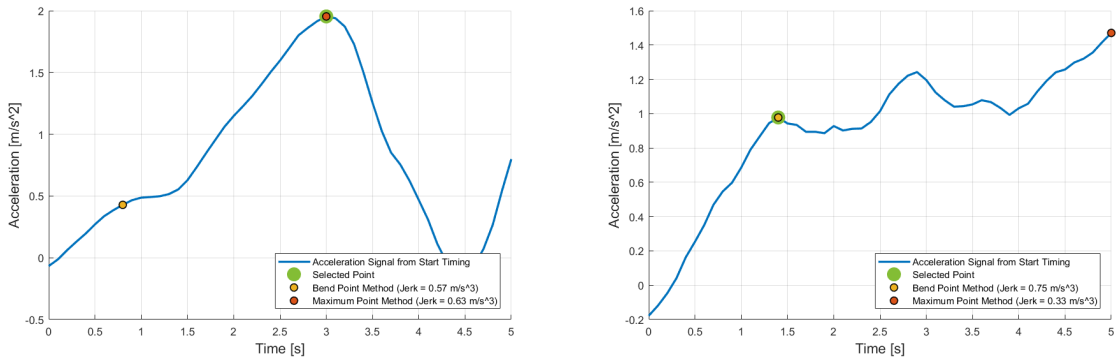

(a) Example of bad detection of the bend point method: maximum point is selected.

(b) Example of bad detection of the maximum point method: the bend point is selected.

Figure 2.6: Possible issues in initial acceleration level detection.

2.4. General Statistics of Data Extractions

Ultimately 55.096 acceleration episodes where extracted from the EuroFOT French data set. To better understand the extracted data the distribution of some of the key parameters are checked. This process is also helpful to verify that the extraction algorithm did not affect negatively the final dataset.

In Figure 2.7a it is possible to see the distribution of ego speed at ego acceleration start. Around 30% of the samples start at standstill, the rest of the cases allow to model the behaviour up to $80 km/h$. As expected, the extraction logic is not able to detect cases at high speeds, this is due to the fact that at high speeds the drivers rarely perform high accelerations since they are smoothly following the lead vehicle in highway conditions. In Figure 2.7b the time delay between the ego and target reaction is shown. It is possible to see that most reactions happen in an interval between 1 and 1.5 seconds. The steps in the cumulative distribution are simply given by the fact that since the data has a frequency of $10 Hz$ the minimum resolution of the delay is of $0.1 s$.

Figure 2.8a shows that many acceleration episodes start at a very short relative distance, even closer than 2 meters. Figure 3.16) confirms that these episodes represent the very low percentiles of the cases starting at very low speed. As discussed above, standstill cases represent 30% of the dataset. Figure 2.8b shows the distribution of relative speed at ego acceleration start, with relative speed being positive when the target is faster that the ego vehicle. A small part of the data set has negative relative speed at ego start, this means that the the ego vehicle was still approaching the target when it started accelerating. In these cases the driver is not reacting to the target vehicle motion but to the scene context (e.g. traffic lights), for this reason these cases were excluded from the analysis. Thanks to the understood context the driver is reacting to the situation and not directly to the lead vehicle. This is also possible to see from Figure 2.7b where the delay of ego reaction is as low as 0.2 seconds. Within this time the human body is not able to process the information and react pressing the accelerator pedal. Finally in Figure 2.9 the distributions of initial ego acceleration and jerk are compared: the distribution of these variables is quite similar both in terms of values and shape. More about this similarity will be studied in Section 3.2.

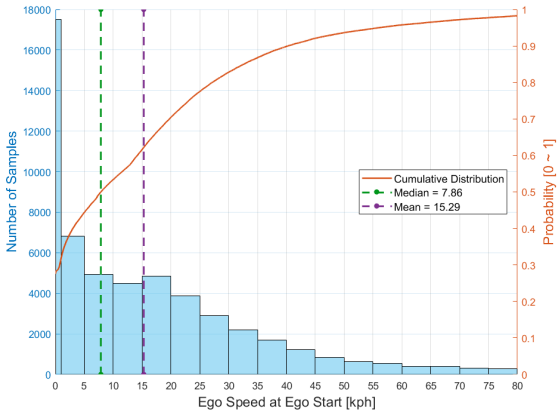

(a) Ego speed at ego start timing.

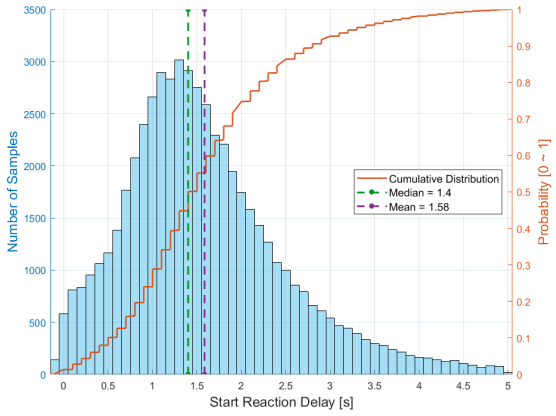

(b) Reaction time between ego and target vehicle.

Figure 2.7: Distribution of the extracted data set: ego speed and reaction delay.

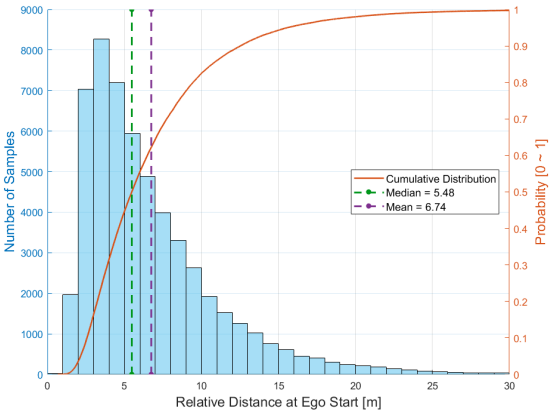

(a) Relative Distance at ego start timing.

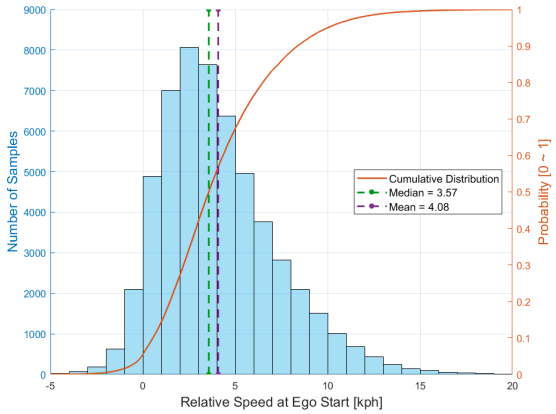

(b) Relative Speed at ego start timing.

Figure 2.8: Distribution of the extracted data set: relative states.

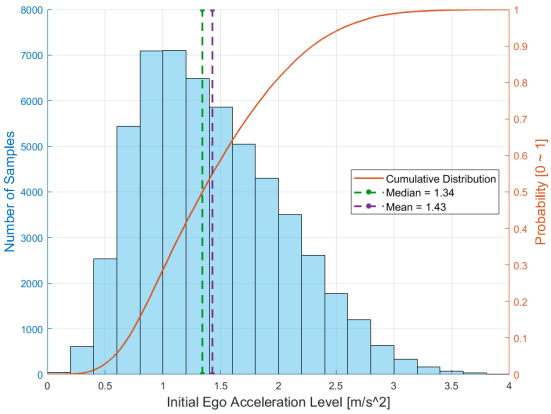

(a) Ego initial acceleration level.

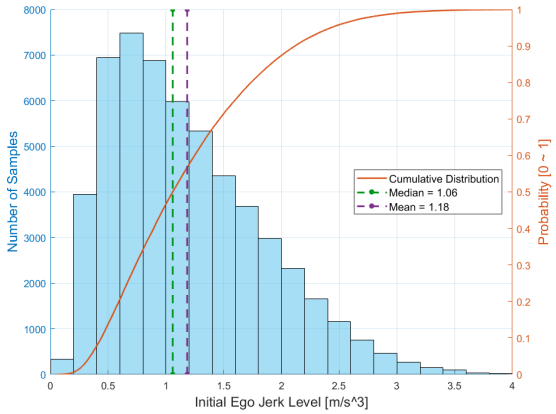

(b) Ego initial jerk level.

Figure 2.9: Distribution of the extracted data set: ego initial acceleration and jerk.

3

Driver Behaviour Models

This chapter will cover the process followed for the creation of the driver behaviour models. Three models are created to model the *following acceleration* scenario: initial acceleration level, initial jerk and start relative distance. Combined, these models define both the most appropriate timing and magnitude of the acceleration event of the ego vehicle. In the creation of this modelling methodology the trade off between complexity and accuracy was always kept in mind. The simplicity of these models allows simpler implementation and evaluation in real vehicles. Nonetheless the accuracy of the model should be kept, making sure that the driver behaviour is accurately modelled.

3.1. Initial Acceleration Level

The first model that will be treated is the initial acceleration level. The objective of this model is to provide an acceleration value based on conditions given by the driving scene and the driving manner. The dependent variable used to create the model was the initial acceleration level previously computed in Section 2.3.

3.1.1. Choice of the independent variables

The main method used to determine the dependency between the different parameters was to bin the independent variable along its range and afterwards check the distribution of the dependent variable within the bin. The impact of various parameters on the acceleration level was checked. The first parameter selected was the ego driving speed at ego start timing. Driving speed is an important parameter as it heavily defines the driving scene in which the acceleration scenario happens. A scenario at stand still will be perceived differently by the driver compared to one at high driving speed.

Another important influence on driver's reaction will be done by the target vehicle's behaviour. Whether the target vehicle accelerates more or less will affect the response of the ego vehicle. The main states influenced by the target vehicle behaviour are relative speed, relative distance and target acceleration. By checking the dependency of these three parameters the relative speed has the clearest influence, on top of that, humans perceive relative speed more easily than target vehicle acceleration. The initial acceleration level was binned both for ego and relative speed, both taken at ego start timing. The 50^{th} percentile of each bin is then plotted in Figure 3.1. Thereby this figure captures the median human response. All bins with less than 75 data points inside of it were discarded.

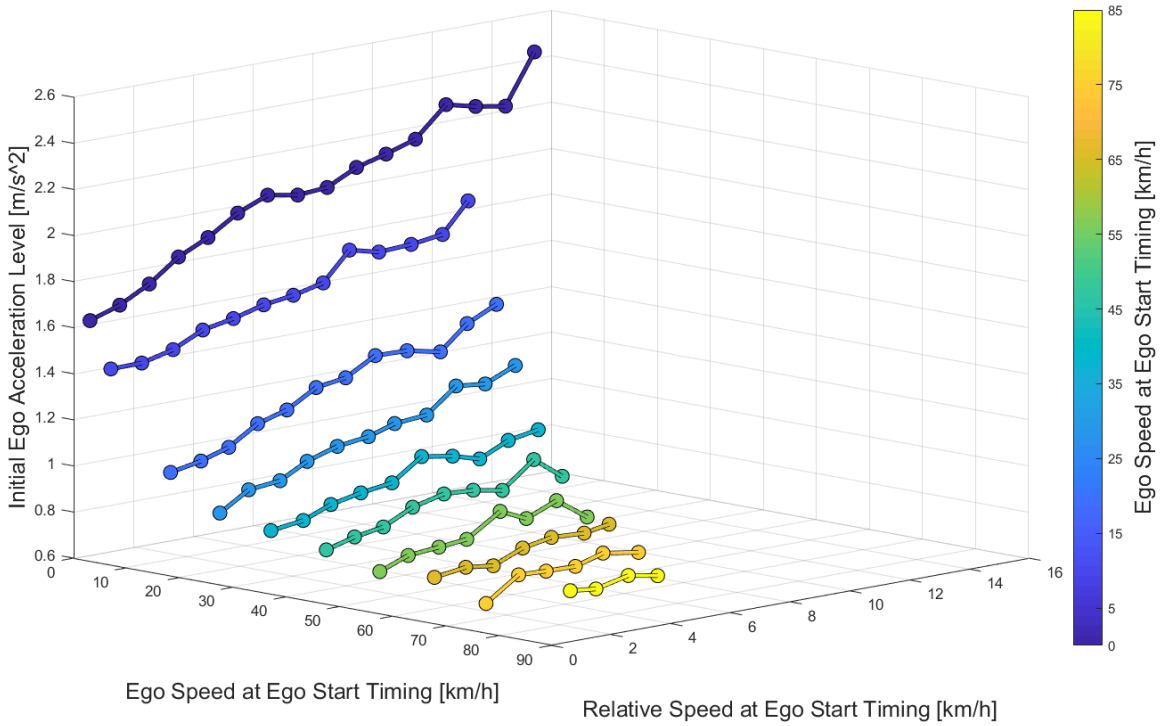

Figure 3.1: Initial acceleration level 50^{th} percentile binned for ego and relative speed.

3.1.2. Fitting the model

Given the points plotted in Figure 3.1 it is now necessary to find a function that can correctly represent the influence of the two independent variables on the initial acceleration level. By analyzing more in detail the separate influence of each parameter it is possible to notice that their effect is not the same. By looking at Figure 3.2a it is clear that the acceleration level decreases rapidly with the increase of ego speed. After doing a trial fitting it was found that an exponential relationship represented the trend of the data more correctly compared with a more traditional polynomial least square regression. On the other hand, in Figure 3.2b it is possible to see that a simple linear fit correctly represents the dependency of the relative speed on the initial acceleration level.

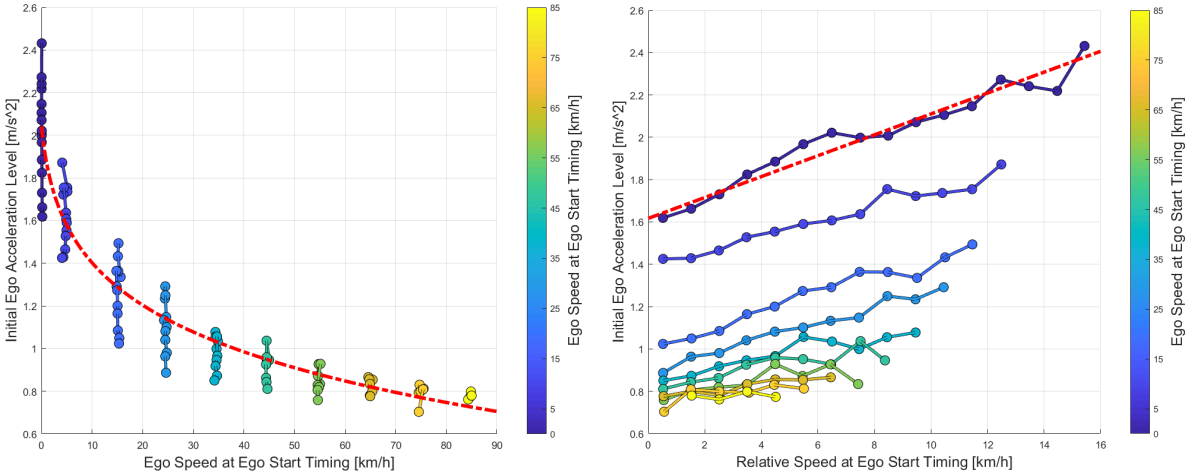

(a) Focus on ego speed dependency.

(b) Focus on relative speed dependency.

Figure 3.2: Initial acceleration level 50^{th} percentile binned for ego and relative speed. (side views)

The main fitting function of the model will have to include both dependencies of the independent variables in one single expression. The first version of the fitting function simply sums the linear correlation of relative speed with the exponential one of ego speed:

$$a_{e,\,initial} = p_1 V_r + p_2 + p_3 V_e^{p_4} \tag{3.1}$$

A limitation of Equation 3.1 was quickly discovered: the slope (p_1) of the linear influence of relative speed was always constant. As it is possible to see in Figure 3.2b the slope changes and gets lower as ego speed increases. In order to include this behaviour in the fitting function the linear and the exponential contribution were multiplied (Equation 3.2). This was able to fit the data correctly but if the ego speed is equal to zero the initial acceleration level will also be zero which is not what the data shows. To solve this issue a constant value of 1 is added to the ego speed (Equation 3.3). This drawback could also be solved by adding a fourth parameter to the fitting. This was taken into consideration but ultimately the gained precision was negligible compare to the simplicity of having one less parameter in the model. In the final version of the fitting function if the speed goes to zero the initial acceleration level is simply given by the linear relationship with relative speed.

$$a_{e,\,initial} = \left(p_1 V_r + p_2\right)(V_e)^{p_3} \tag{3.2}$$

$$a_{e,\,initial} = \left(p_1 V_r + p_2\right)(V_e + 1)^{p_3} \tag{3.3}$$

In Figure 3.3 it is possible to see the final function fitted to the initial acceleration 50^{th} percentile, the function is able to correctly follow the trends of the data. In order to make sure that the function works correctly for the full driving behaviour range, the fitted function is also plotted for the 10^{th} and 90^{th} percentile. The result is visible in Figure 3.4.

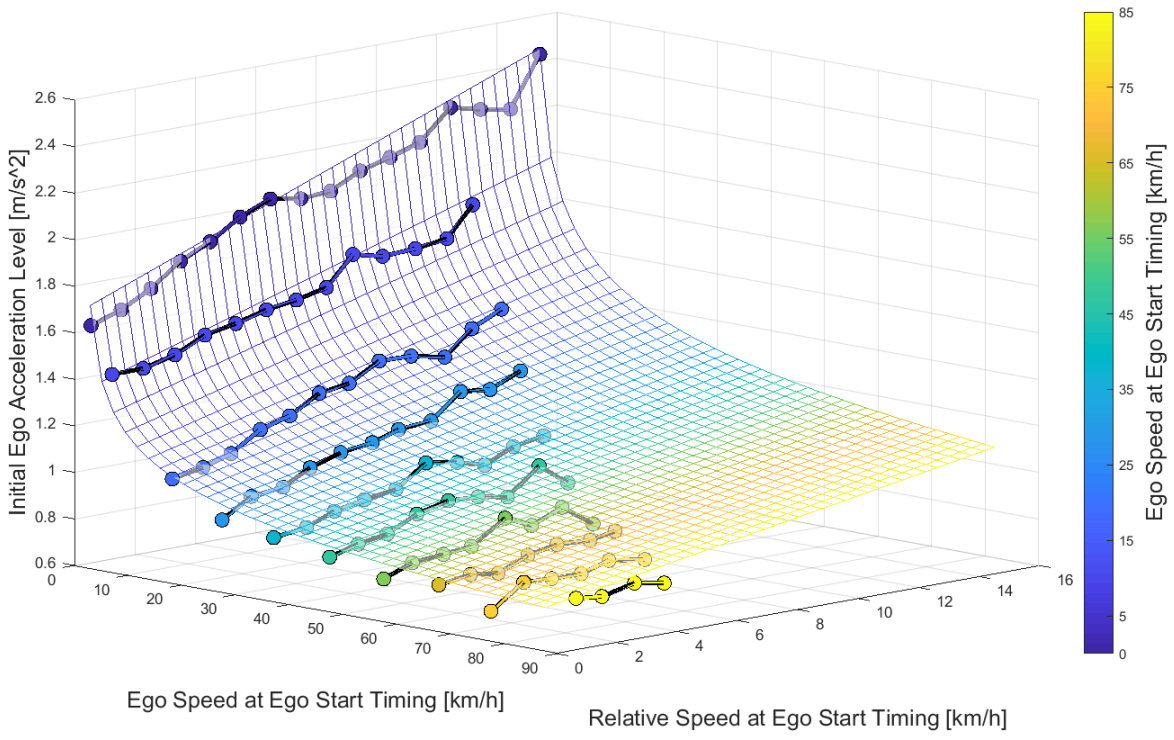

Figure 3.3: Fitting of Initial acceleration level 50^{th} percentile binned for ego and relative speed.

Now that a correctly working function is found it is possible to continue in the final fitting of the driver behaviour model. Firstly the selected function is fitted for each Acceleration Percentile from

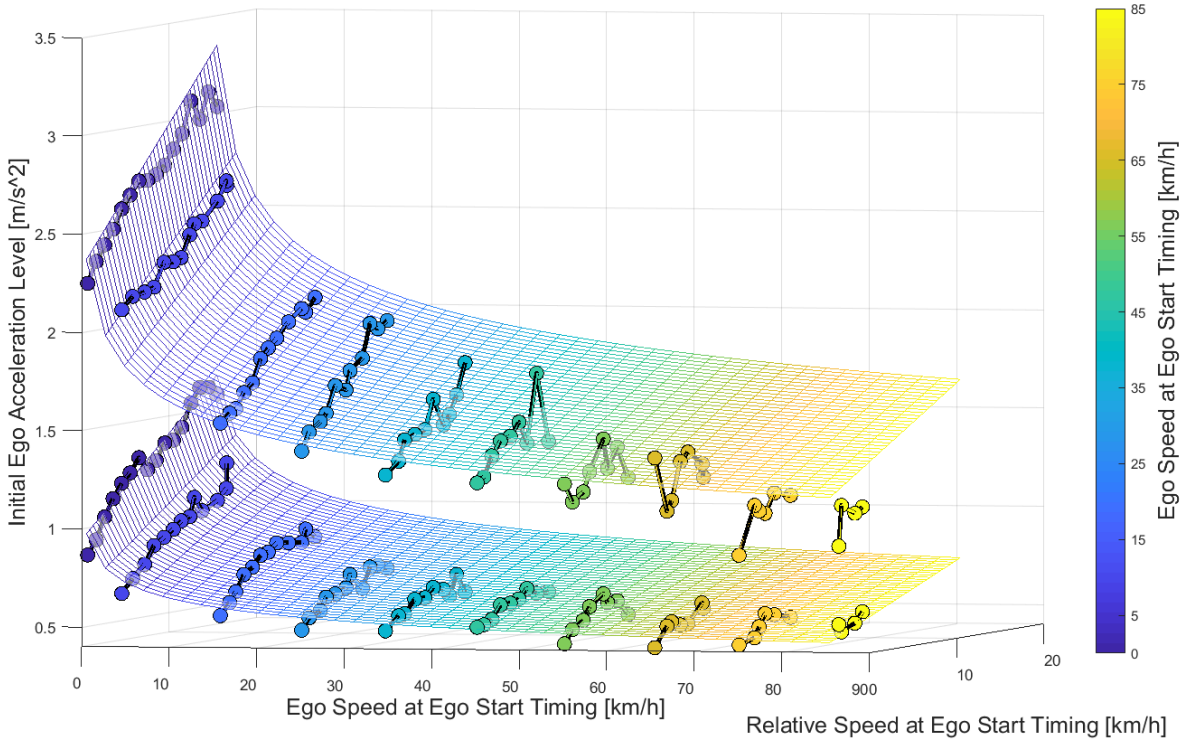

Figure 3.4: Fitting of Initial acceleration level 10^{th} and 90^{th} percentile binned for ego and relative speed.

the 10^{th} to the 90^{th}. The goodness of each fit is shown in Figure 3.5 (blue points) in terms of both R-squared (Figure 3.5a) and RMSE (Root Mean Square Error) (Figure 3.5b). Overall the accuracy of all fit is very high, as expected some precision is lost for very high and very low percentiles nonetheless the RMSE remains lower than 0.1 m/s^2 and the R-square higher than 0.97. The result of this fitting process is a set of three parameters (p_1, p_2 and p_3) specifically optimized for a particular percentile. This corresponds to a total of 240 different parameters which is an unpractical amount for an eventual implementation of the model. In order to simplify the model, the optimized parameters, plotted in Figure 3.6 (blue points), are fitted by means of linear regression as a function of the Acceleration Percentile. The resulting fitted functions are shown in Figure 3.6 (red lines). The exponent parameter p_3, shown in Figure 3.6c, was ultimately kept constant in function of Acceleration Percentile. It was quickly noticed that applying the linear fitting to the parameter was not increasing the accuracy of the model by much. Keeping the exponent constant greatly simplifies the mathematical operations necessary to formulate the model in a practical matter. More about the mathematical steps will be covered in Section 3.1.3. Finally, the accuracy of the fit is computed again accounting for the fact that the parameters are estimated with the linear regression. The results are shown in Figure 3.5. Comparing the results to the ones obtained with the optimized parameters shows that not much accuracy is lost, especially in the range between the 20^{th} and the 80^{th}. The R-square values are still above 0.92 and the RMSE ones are still below 0.16 m/s^2, the accuracy lost is considered acceptable.

3.1.3. Model Formulation

Now all the parameters necessary to produce a final formulation of the model are known. Firstly, the fitting function seen in Equation 3.3 is rewritten in a matrix form in the following manner:

$$a_{e,initial} = \begin{bmatrix} p_1 \\ p_2 \end{bmatrix}^T \begin{bmatrix} V_r\,(V_e+1)^{p_3} \\ (V_e+1)^{p_3} \end{bmatrix} \implies a_{e,initial} = \underline{p}^T \underline{V} \tag{3.4}$$

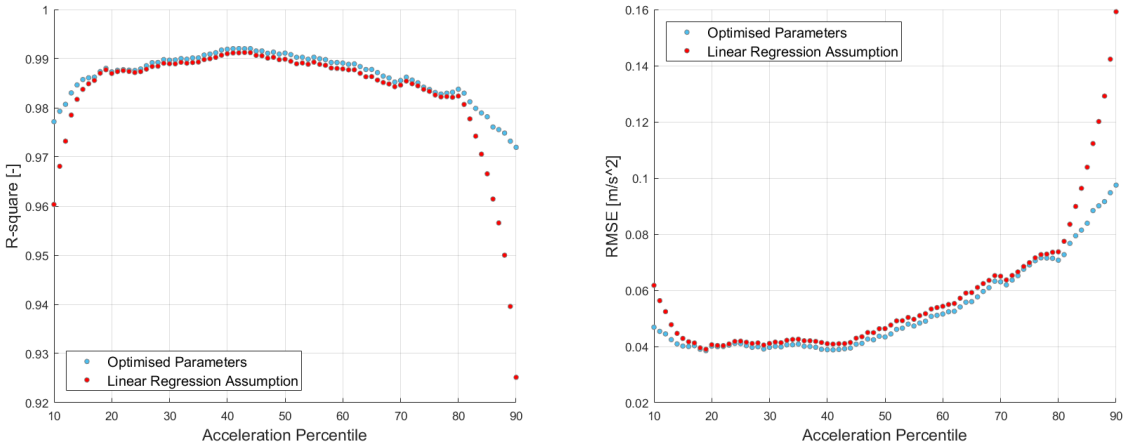

(a) R-squared values of the initial acceleration model fitting.

(b) RMSE values of the initial acceleration model fitting.

Figure 3.5: Goodness of fit of the initial acceleration model.

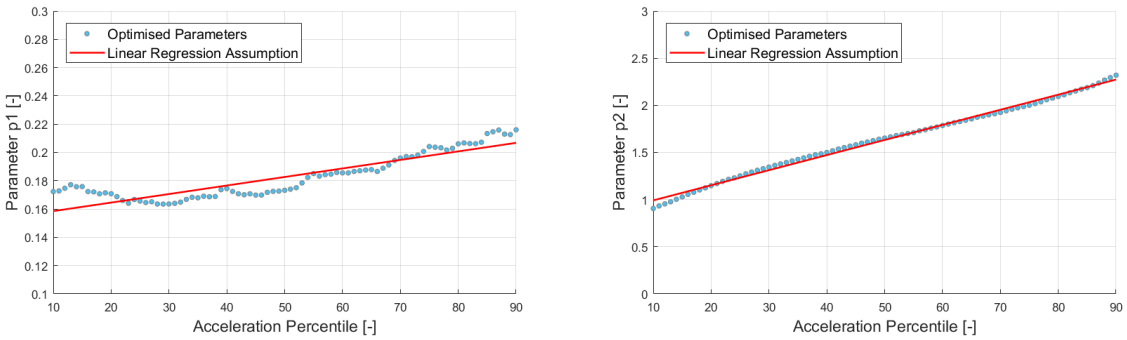

(a) p_1 parameter as a function of the Acceleration Percentile

(b) p_2 parameter as a function of the Acceleration Percentile

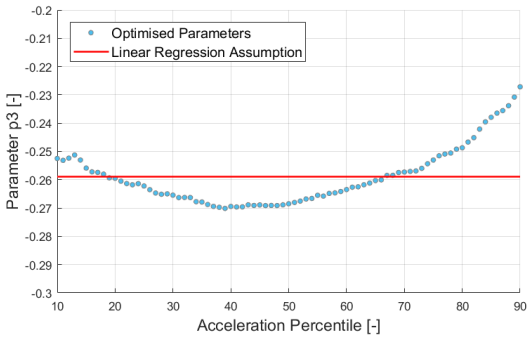

(c) p_3 parameter as a function of the Acceleration Percentile

Figure 3.6: Fitting parameters of initial acceleration model as a function of the Acceleration Percentile.

Where $\underline{p}$ is the vector of the parameters and $\underline{V}$ is the vector of the vehicle states. Here it is already possible to appreciate one of the benefits of keeping the parameter p_3 constant. If p_3 is not constant it would not be possible to explicitly separate the parameters vector from the vehicle states one, hence the next steps would have to be done recursively.

In the previous section the other parameters (p_1, p_2) were linearly fitted as a function of the

Acceleration Percentile, this dependency is also written in a more compact vector form in Equation 3.5. Where $\underline{\alpha}$ and $\underline{\beta}$ are the vectors containing the parameters of the linear regression. By plugging the resulting expression from Equation 3.5 into Equation 3.4, the two possible formulations of the model are found: one with the initial acceleration level as the output and the other with the acceleration percentile as the output. They can both be found in Equation 3.6.

$$\begin{cases} p_1(AP) = \alpha_{p_1} AP + \beta_{p_1} \\ p_2(AP) = \alpha_{p_2} AP + \beta_{p_2} \end{cases} \implies \underline{p} = \underline{\alpha} AP + \underline{\beta} \tag{3.5}$$

$$a_{e,\,initial} = \left(\underline{\alpha}^T AP + \underline{\beta}^T\right) \underline{V} \iff AP = \frac{a_{e,\,initial} - \underline{\beta}^T \underline{V}}{\underline{\alpha}^T \underline{V}} \tag{3.6}$$

It is now possible to highlight the main benefit of this type of models. Not only is it possible to compute the corresponding acceleration level to a certain driver percentile, but it is also possible to do the inverse process: given an acceleration level it is possible to check the percentile it corresponds to.

$$a_{e,\,initial} = f\left(V_e,\, V_r,\, AP\right) \iff AP = f\left(V_e,\, V_r,\, a_{e,\,initial}\right) \tag{3.7}$$

3.1.4. Model Validation & Correction for Target Acceleration

Before proceeding with the development of the model it is necessary to check how accurate the model is, and if all the main influences on driver behaviour are correctly modeled. First, using the model in Equation 3.6, the AP value is computed for every acceleration episode. Subsequently the AP was binned for different parameters and for each bin different percentiles were computed. This was done in order to check that the model correctly represents the influence of the modelled parameters and whether other parameters influence it or not. In Figure 3.7 the dependency of the two independent variables of the model on AP is plotted. Ideally, if the fitting of the model was perfect at every percentile, in these figures the lines would be perfectly horizontal as the influences of ego and relative speeds are perfectly modelled. Due to the various assumptions made throughout the creation of the model these lines have small fluctuations but overall they are quite constant. As could be seen in the fit performance, in these plots it is also clear that the precision of the model decreases as the distance from the 50^{th} increases.

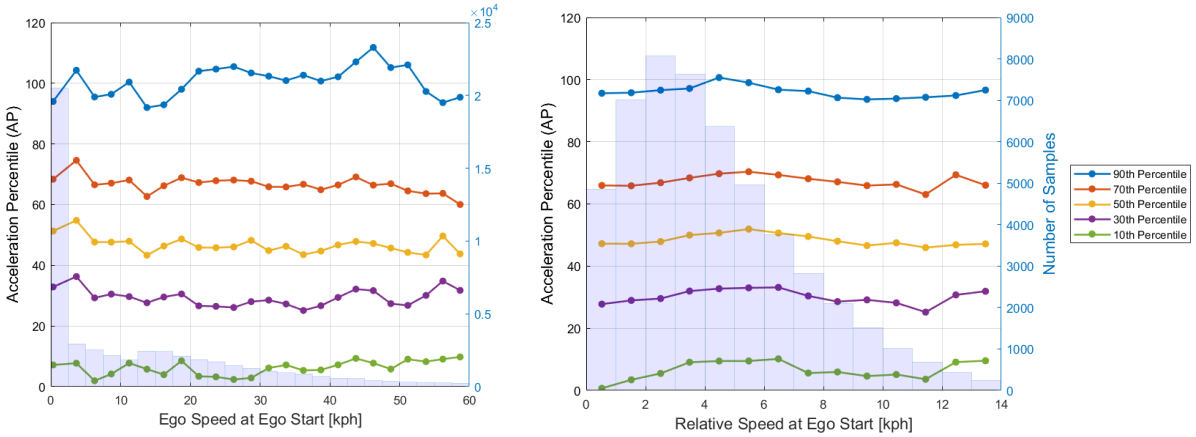

(a) AP binned for ego speed.

(b) AP binned for relative speed.

Figure 3.7: Initial acceleration model validity verification (left scale: acceleration percentile, right scale: amount of datapoints per bin).

At this stage the influence of other parameters is also checked. This is done to make sure that all the necessary independent variables are included in the model. Out of the checked driving scene parameters the only one that had a clear influence on AP was the Target Acceleration at Ego Start. Reasonably, the magnitude of the target vehicle's acceleration has a direct influence on the acceleration level of the ego vehicle. This was also found in literature in the research of Sultan et al. [40]. In Figure 3.8 it is clearly visible that the target acceleration has a linear influence on the AP.

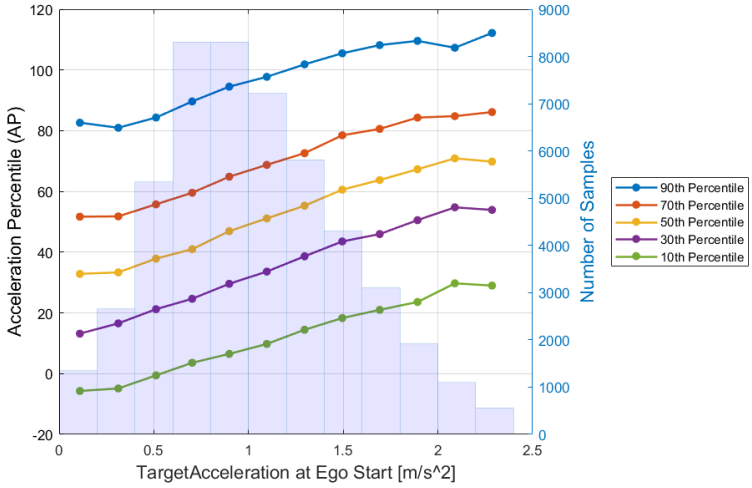

Figure 3.8: Acceleration Percentile (AP) binned for target acceleration at ego start timing.

This dependency cannot be ignored, for this reason it will be introduced in the model. Rather than performing a four dimensional regression which would have overly complicated the model, the AP value is simply corrected with the following linear correlation:

$$AP^* = AP - \sigma a_t \tag{3.8}$$

Where σ is the slope of the linear dependency and a_t is the target acceleration level. By inserting the expression in Equation 3.7 the new expressions of the model are found:

$$a_{e,\,initial} = \left(\underline{\alpha}^T \left(AP^* + \sigma a_t\right) + \underline{\beta}^T\right)\underline{V} \iff AP^* = \frac{a_{e,\,initial} - \underline{\beta}^T \underline{V}}{\underline{\alpha}^T \underline{V}} - \sigma a_t \tag{3.9}$$

Now using the second expression of Equation 3.8 the AP^* value can be calculated but unfortunately, due to the model inaccuracies and the final correction for the target acceleration, the AP^* value no longer represents an exact estimation of the driving percentile. In the next section the model is finalized with the conversion of the AP^* value in *aggressiveness*.

3.1.5. Conversion to *Aggressiveness*

At this stage the values of AP^* calculated back from the acceleration episodes of the data set have lost the meaning of data percentile. This is because of the inaccuracies of the model and the target acceleration correction. The aim of this final step is to convert the AP^* back to a value between 0 and 100 that will be called *aggressiveness*.

If the distribution of AP values is inspected (Figure 3.9a) it is possible to see that the back-calculation of the model led to some unusual values: both smaller than 0 and higher than 100. This not only due to the imperfection of the fit but also due to the fact that the model was fitted between the 10^{th} and the 90^{th} percentile as it is not the intent of this modelling process to grasp very extreme driving behaviour but rather to accurately model the average variations in it. The distribution of the

corrected AP^* values in Figure 3.9b shows that the amount of unusual values only grows with the introduction of the third independent variable: the target acceleration. In this case the median of the data shifts from 50 to 25.

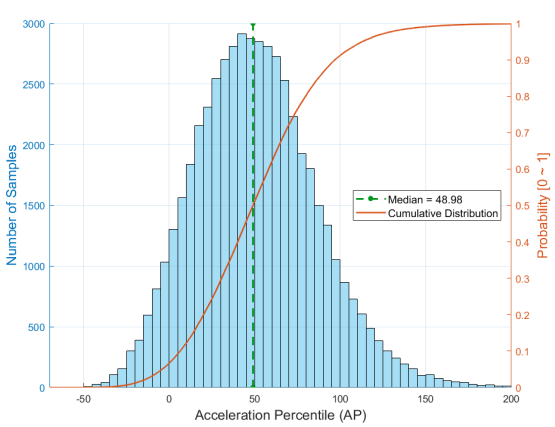

(a) Distribution of Acceleration Percentile (AP)

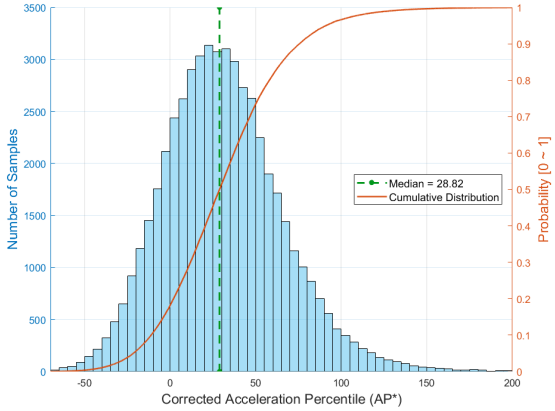

(b) Distribution of Corrected Acceleration Percentile (AP*)

Figure 3.9: Comparison of the distributions of the corrected and non corrected acceleration percentiles

In order to convert the AP^* values into *aggressiveness* the distribution in Figure 3.9b is fitted to a known distribution. By taking the Cumulative Distribution Function (CDF) of the fitted distribution this will return a value between 0 and 1 for every AP^* based on how aggressive the driver was in that scenario. The distribution of AP^* is both fitted to a Normal distribution and a Generalized Extreme Value (GEV) distribution, the results are compared in Figure 3.10. Although both types of distributions can correctly fit the AP^* values, the Normal distribution was chosen being the most common type of distribution. In this case, the data fitted had an almost perfectly symmetric distribution, but this is not always the case when modelling driver behaviour. For example, in the first chapters when checking the distribution of the extracted data it was possible to see that the distribution like the relative distance at ego start timing (Figure 2.8a) had a very asymmetric CDF. This is given by the fact that very high values of relative distance are still possible, whilst very low ones are limited by the possibility of collision between the vehicles. During the modelling of the acceleration start distance (Section 3.3) it will be possible to see the benefits of the GEV distribution.

Now that the final step of the model is complete it is possible to once again compute the validation plots to verify that the changes to the model didn't influence its accuracy. In Figure 3.11 it is possible to see that the *aggressiveness* value is almost constant in function of the three independent variables, being very close to the respective percentile value. This means that not only the third independent variable is correctly modelled but also that the correction did not affect the accuracy of the influence of ego and relative speed.

With the final model it is now possible to compute the acceleration level from an *aggressiveness* value (from 0 to 100) and, vice versa, given an acceleration level it is possible to determine which is the corresponding *aggressiveness* value. As explained in the beginning, this type of model allows for a flexible tuning procedure when the model is implemented in a real vehicle. A visual representation of the model can be seen in Figure 3.12.

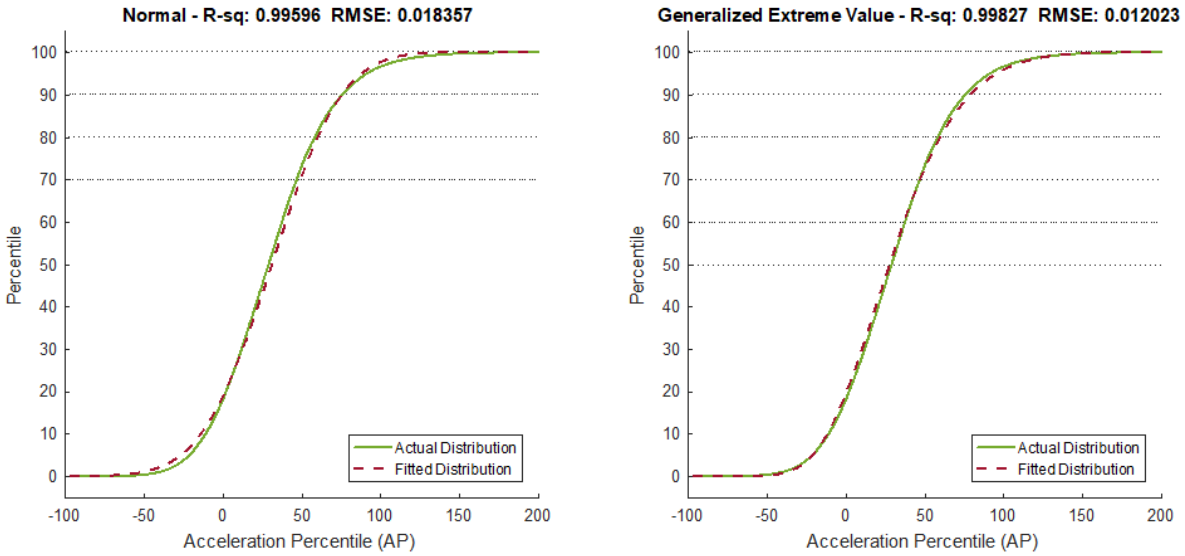

Figure 3.10: Comparison of fitted distributions.

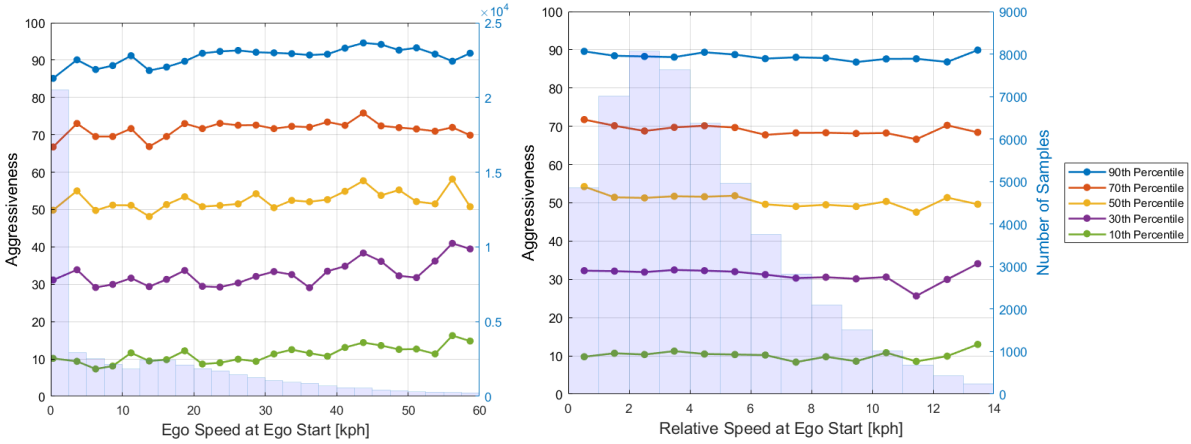

(a) *Aggressiveness* binned for ego speed.

(b) *Aggressiveness* binned for relative speed.

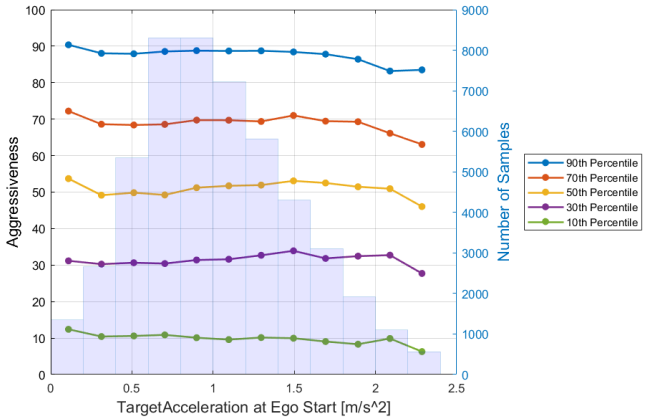

(c) *Aggressiveness* binned for target acceleration.

Figure 3.11: Initial acceleration model final validity verification.

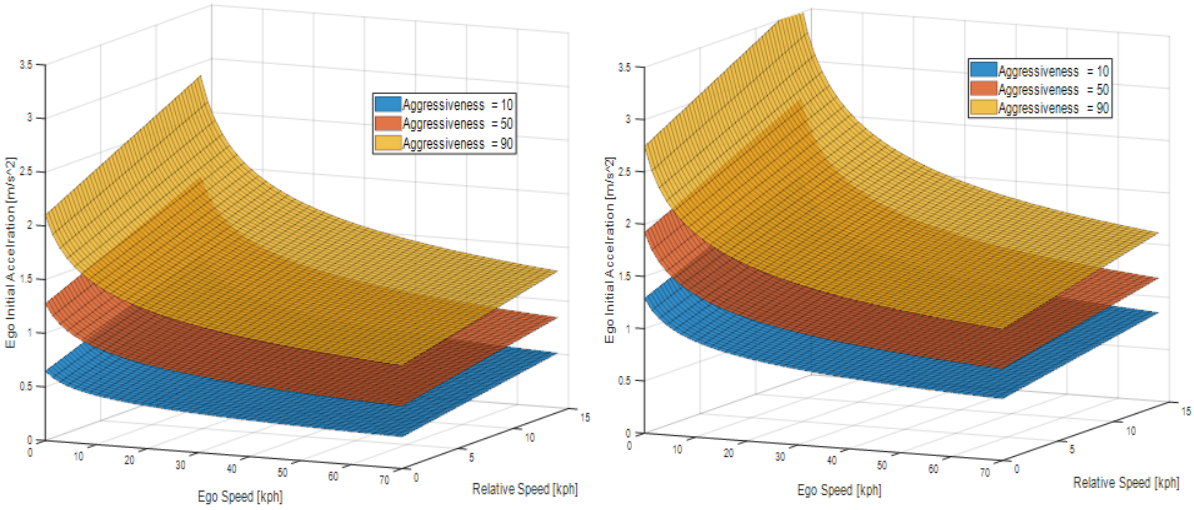

(a) Acceleration model for target acceleration $0 m/s^2$ (b) Acceleration model for target acceleration $2 m/s^2$

Figure 3.12: Visualization of final acceleration level model.

3.2. Initial Jerk

Now that the acceleration level used by the drivers is modelled, in order to characterise a realistic acceleration profile, the modelling of jerk needs to be included. This is a necessary step in order to understand at what comfortable rate the acceleration level can be achieved. Estimating the exact jerk value is not as critical as estimating the acceleration level, for this reason it was chosen to follow a much simpler modelling approach compared to the *aggressiveness* method used in the acceleration model. This model will not vary with the changing of driving style but will only be influenced by the driving condition. Using this approach it is possible to have a realistic image of the jerk value without having to deal with a complicated model, facilitating the implementation of the model in a possible logic.

It is important to remark that the jerk value modeled in this chapter is the average jerk associated with the extracted initial acceleration value explained in Section 2.3. During the development of the initial acceleration model, the influence of the driving scene on the driving behavior was checked. For example, in the previously shown Figure 3.2a, the influence of ego speed at ego start timing on the initial acceleration is inspected. This process was also followed for the initial jerk and it was quickly clear that the driving condition influence on the jerk value was very similar to the one on the initial acceleration level. As it's possible to see in Figure 3.13 the effect of relative speed and ego speed on the two variables follows the same trends. For this reason, the possibility of creating a simpler model is investigated. Instead of also taking into consideration in this case the *aggressiveness* of the driver, this model will define just the correlation between initial jerk and initial acceleration level.

In Figure 3.14 it is possible to see how all the acceleration events are distributed in the acceleration - jerk plane, where the coloured lines represent the percentage of data set enclosed in the contours. By looking at how the data is distributed, a trend is clearly visible: the higher the acceleration level the higher the corresponding jerk level. This correlation is probably given by the fact that the driver is willing to increase the acceleration quicker when a high level of acceleration is required. This is likely done by the driver in order to achieve a faster reaction to a high accelerating target vehicle. The data set is fitted using a linear regression method that minimizes the orthonormal distance between the points and the data. The final result is visible in Figure 3.15 and the expression of the fitting is written as follows:

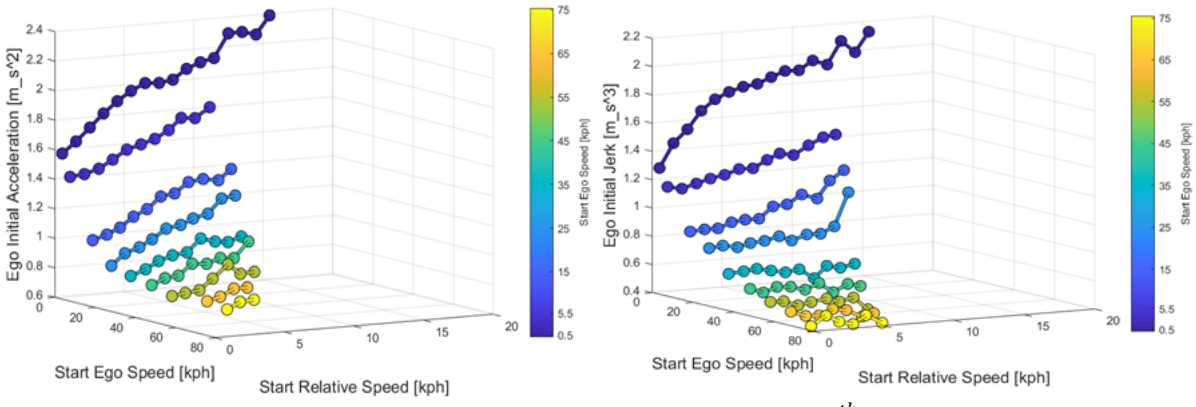

(a) Initial acceleration level 50^{th} percentile.

(b) Initial jerk level 50^{th} percentile.

Figure 3.13: Comparison of the effect of ego and relative speed on initial acceleration and jerk.

$$j_{e,\,initial} = 1.07\; a_{e,\,initial} - 0.35 \tag{3.10}$$

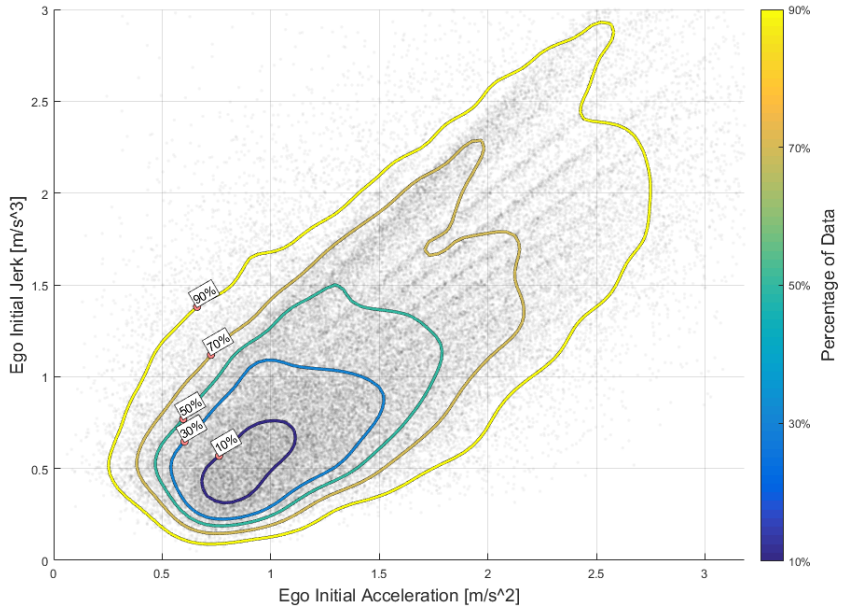

Figure 3.14: Distribution of all acceleration events in the acceleration - jerk plane.

Since the model would output negative jerk values in cases of very low initial acceleration, the model is limited between the 10^{th} and 90^{th} percentile of initial acceleration as outside this range there is not enough data to assess the validity of the model, this limitation of validity can also be seen in Figure 3.15. The final model, despite being simple, can be used to estimate the allowable jerk in the acceleration scenario. This is a very critical part of the acceleration control of a vehicle, as the acceleration changes cannot be instantaneous, a proper level of jerk must be ensured in order to achieve appropriate driver comfort.

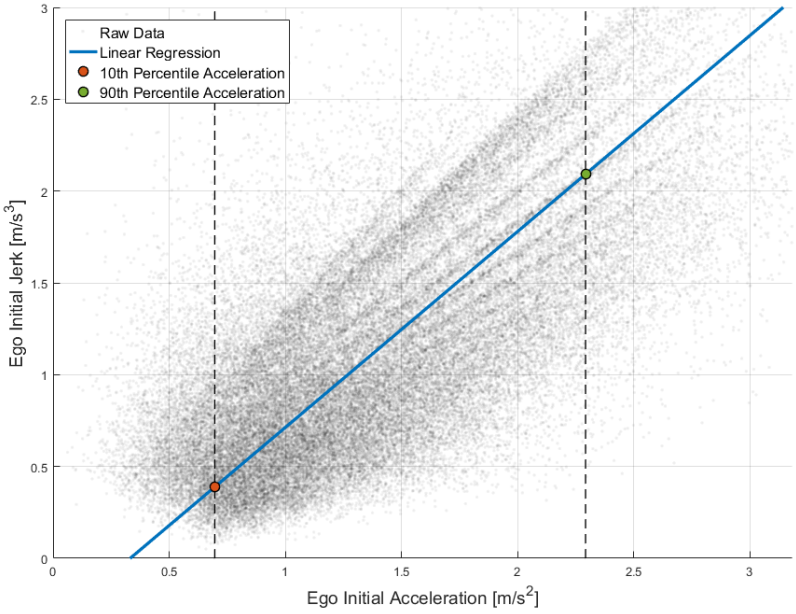

Figure 3.15: Final regression model and model limitations

3.3. Start Relative Distance

Now the full driver reaction is modelled. The remaining portion of the driving scene that still needs to be modelled is the start timing of the ego reaction. In which conditions is the driver willing to start the acceleration reaction? The modelled variable that represents the driver behaviour is the relative distance at ego start. The time delay of the reaction was also taken into consideration as the driver behaviour variable, ultimately it was discarded as the relative distance facilitates the implementation of the model into a working logic: detecting online the start trigger of the delay may be challenging.

If the target vehicle has accelerated far enough then the ego vehicle is comfortable to start accelerating. Regarding the driving scene, many variables were checked in order to see which ones had the biggest influence. Ego speed at ego start had the most significant influence, for this reason it was chosen as driving scene variable. In Figure 3.16 it is possible to see the influence of the ego speed on the driver behaviour, the higher the speed, the higher the start distance. This trend is also influenced by the fact that, at higher speeds the *following distance* is already higher as drivers want to keep a bigger safety margin. The methodology used to create the model is the same used for the initial acceleration level model (Section 3.1). In this case the steps will be simpler as the model has only one input. As for the initial acceleration model, the variation in driving behaviour is included in the *aggressiveness* parameter.

3.3.1. Model Fitting & Formulation

Compared to the initial acceleration model the choice of the fitting function is much simpler. A polynomial quadratic expression (Equation 3.11) is chosen in order to fit the data. As can be seen in Figure 3.17a the function successfully fits the data from the 10^{th} to the 90^{th} percentile. In Figure 3.17b the relative distance values are also displayed in terms of THW, is possible to see that, at higher speed, THW is almost constant.

$$D_r = p_1 V_e^2 + p_2 V_e + p_3 \tag{3.11}$$

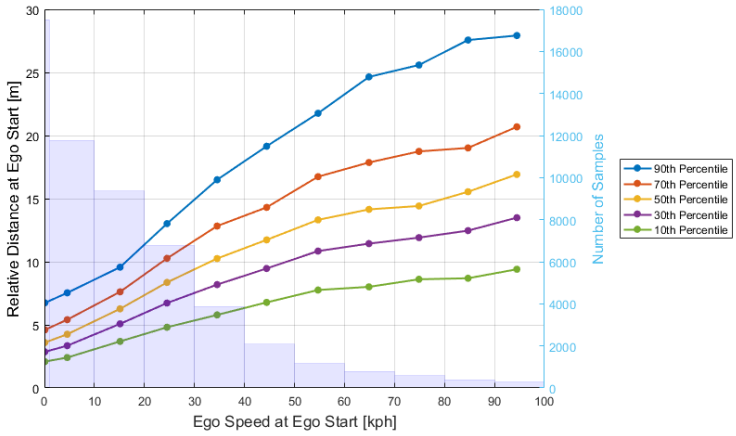

Figure 3.16: Relative distance at ego start timing binned for ego speed at ego start timing.

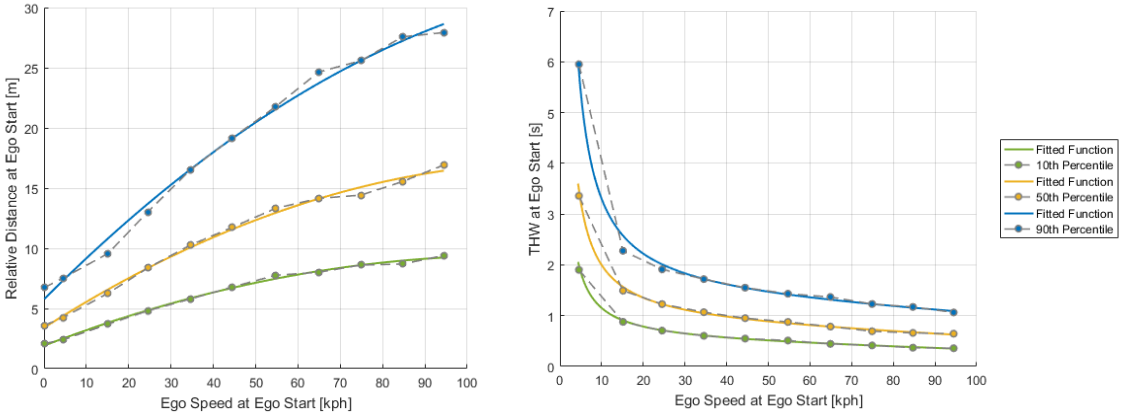

(a) Fitting of relative distance values.

(b) Relative distance values and function converted in THW.

Figure 3.17: Fitting of relative distance at ego start timing binned for ego speed at ego start timing.

As was done for the initial acceleration level model the first step towards the construction of the model can be performed: the function is fitted to every percentile from the 10^{th} to the 90^{th}. Also for this model the amount of parameters is reduce by fitting linearly the optimized parameters in function of the distance percentile. The resulting parameters together with the linear fitting are shown in Figure 3.18. The goodness of the fit is assessed both in terms of R-square and RMSE. The results are visible in Figure 3.19, both for the optimized parameters and for ones estimated by linear regression. Also for this model the final results of the linear regression simplification are very positive. In this case the precision is lost not only for the very low and very high percentile but also for the central values close to the 50^{th}, nonetheless, the performance is still good with R-square values above 0.93 and a maximum RMSE value of only 2.3 meters.

The model formulation is very similar to the initial acceleration model. The first step is rewriting the fitting function (Equation 3.11) into the following matrix form:

$$D_r = \begin{bmatrix} p_1 \\ p_2 \\ p_3 \end{bmatrix}^T \begin{bmatrix} V_e^2 \\ V_e \\ 1 \end{bmatrix} \implies D_r = \underline{p}^T \underline{V} \tag{3.12}$$

Where the vector $\underline{p}$ contains the fitting parameters and vector $\underline{V}$ the vehicle states, with the latter

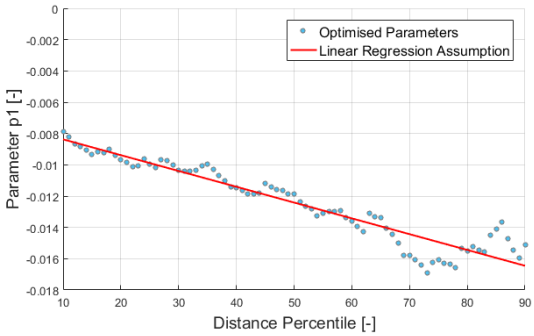

(a) p_1 parameter as a function of the Distance Percentile

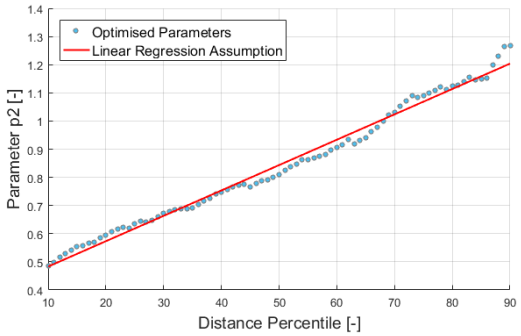

(b) p_2 parameter as a function of the Distance Percentile

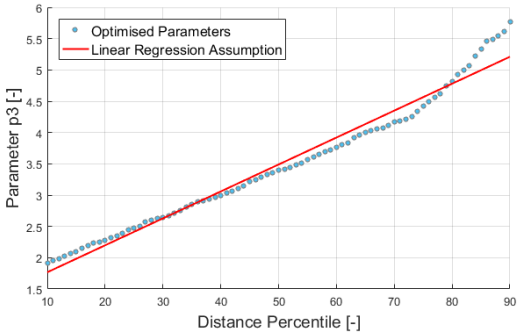

(c) p_3 parameter as a function of the Distance Percentile

Figure 3.18: Fitting parameters of relative distance model as a function of the Distance Percentile.

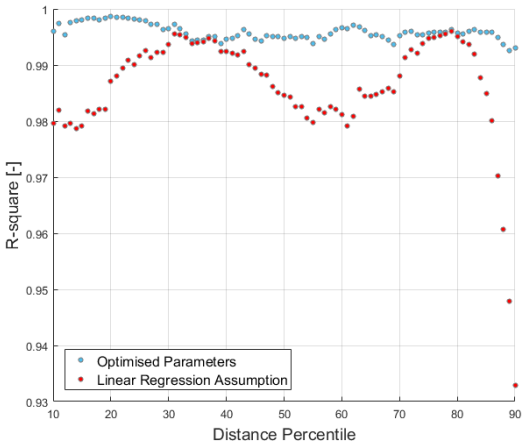

(a) R-squared values of the relative distance fitting.

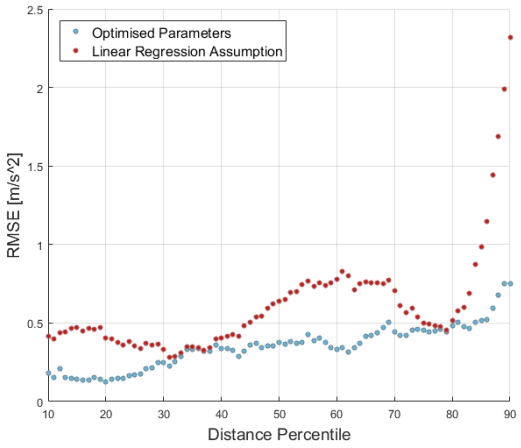

(b) RMSE values of the relative distance fitting.

Figure 3.19: Goodness of fit of the relative distance model.

in this case only referring to the ego speed. In Equation 3.13 also the linear fitting of the optimized parameters are written in a more compact matrix form. Where $\underline{\alpha}$ and $\underline{\beta}$ are the vectors containing the parameters of the linear regression. Lastly by combining Equations 3.12 and 3.13, the two possible final expressions for the model are obtained in Equation 3.14. In the first one the start distance of reaction can be computed from the ego vehicle speed and the Distance Percentile. In the second model formulation, from an acceleration scenario it's possible to compute the corresponding

percentile to the recorded reaction distance.

$$\begin{cases} p_1(DP) = \alpha_{p_1} DP + \beta_{p_1} \\ p_2(DP) = \alpha_{p_2} DP + \beta_{p_2} \\ p_3(DP) = \alpha_{p_3} DP + \beta_{p_3} \end{cases} \implies \underline{p} = \underline{\alpha} DP + \underline{\beta} \tag{3.13}$$

$$D_r = \left(\underline{\alpha}^T DP + \underline{\beta}^T\right) \underline{V} \iff DP = \frac{D_r - \underline{\beta}^T \underline{V}}{\underline{\alpha}^T \underline{V}} \tag{3.14}$$

3.3.2. Conversion to *Aggressiveness* & Validation

The final step of the creation of the model is the conversion of the Distance Percentile into *aggressiveness*. From each acceleration episode the corresponding DP value is calculated using Equation 3.14. In Figure 3.20 it is possible to see how this value is distributed.

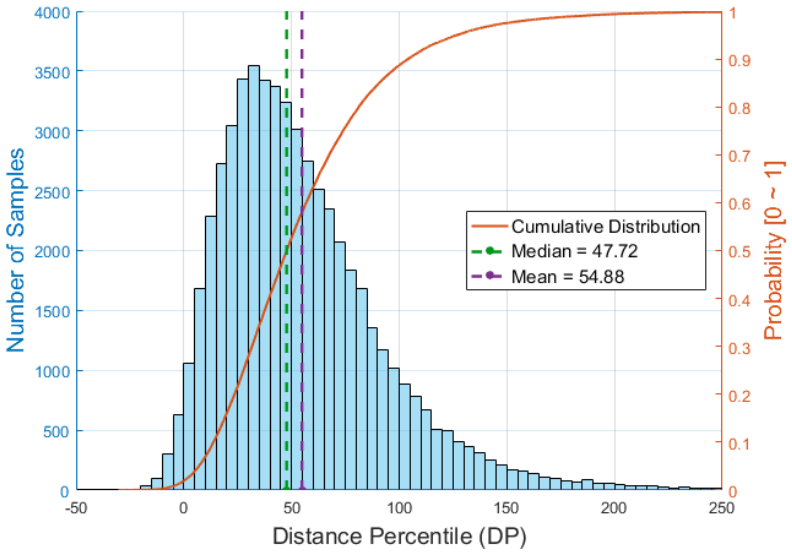

Figure 3.20: Distribution of Distance Percentile (DP).

As expected, some values of DP are outside the 0 to 100 range due to the fitting inaccuracies. As was done for the initial acceleration model, the DP values are converted into values ranging from 0 to 100 called *aggressiveness*. This operation is done by fitting the DP distribution to a known distribution. In Figure 3.21 the resulting fitting to both a normal and GEV distribution is shown. As explained in Section 3.1.5, often when modelling driver behaviour the variables are not distributed in a symmetric manner. The relative distance is a good example of it as low values are limited by the risk of collision but very high values are still possible. Since the fitting performance is almost perfect, the GEV distribution is chosen. Since a high percentile corresponds to a high distance value it means that the least aggressive drivers will keep a bigger margin when accelerating. For this reason, the DP value is converted by taking 1-CDF so that a high percentile corresponds to a low *aggressiveness*. The final visualization of the model can be seen in Figure 3.22. Lastly, the model is validated by checking if the influence of the driving condition is correctly represented by the model. In Figure 3.23 the *aggressiveness* is plotted in function of the driving condition: ego speed at ego start timing. Clearly the model is able to estimate *aggressiveness* independently of the driving condition as the plotted lines are constant.

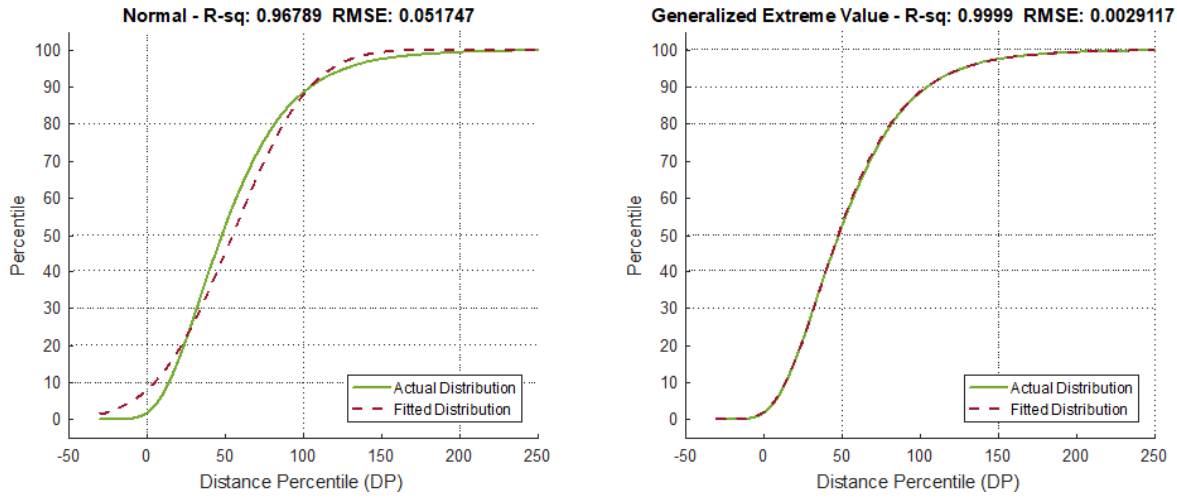

Figure 3.21: Comparison of fitted distributions.

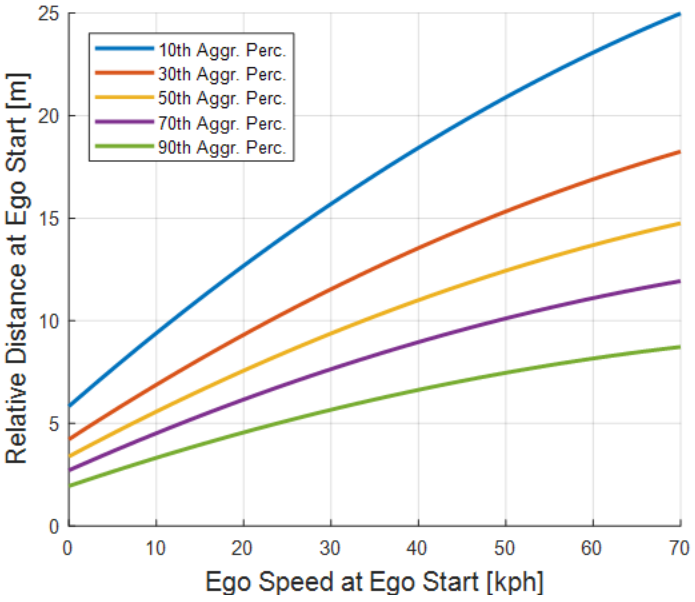

Figure 3.22: Visualization of final relative distance model.

3.4. Correlation Between the Models

Once all the models are created is possible to check if there is any correlation between them. In particular if the initial acceleration model and the start relative distance model represent aggressive and conservative behaviour at the same time. Does a driver that keeps a short distance to the preceding vehicle also accelerate stronger than average? In Figure 3.24 is possible to see that this is not necessarily the case. Here the start relative distance *aggressiveness* is plotted against the initial acceleration *aggressiveness*. Overall the percentile lines are almost flat apart from a slightly positive slope of the 50^{th} percentile line. If the influence would have been greater it would have been possible to combine the two models and reduce even further the number of required parameters to represent driver behaviour.

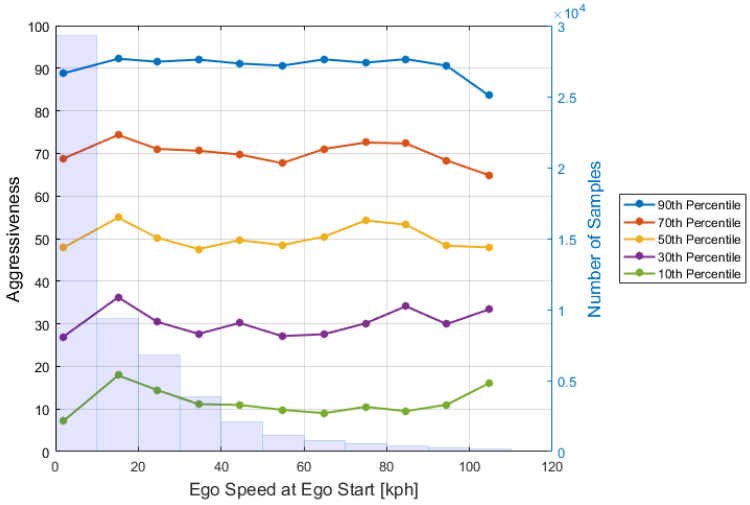

Figure 3.23: Relative distance model validity verification.

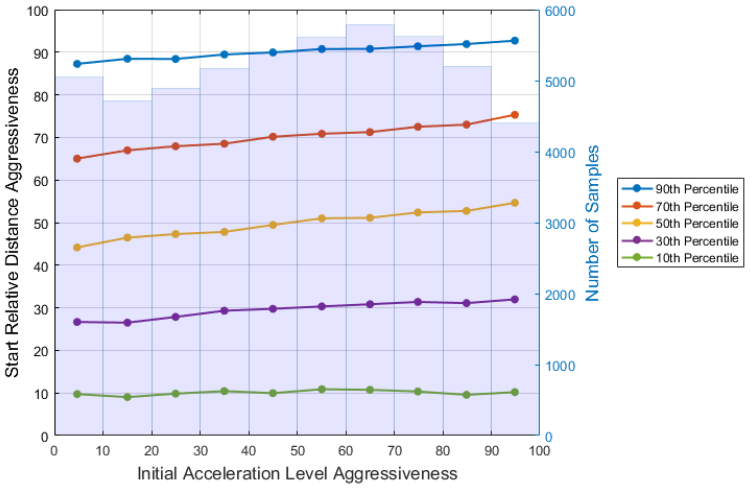

Figure 3.24: Correlation between initial acceleration *aggressiveness* and initial relative speed *aggressiveness*.

4

Simulation

In this chapter, two examples of the implementation of the driver behaviour models developed in the previous chapter are shown. The models are simulated and compared to a current Toyota ACC logic, highlighting the potential shortcomings of the system in the acceleration during *following* behaviour. All simulations mentioned in this chapter were performed using the Simulink simulation environment.

4.1. Implementation of driver behaviour models

The three driver behaviour models explained in Chapter 3 characterize how the driver reacts when following a lead vehicle accelerating. This is done by modelling three main variables: initial acceleration, initial jerk and relative distance at reaction start. At this stage, models represent only the fitted formulas already explained in Chapter 3. In order to simulate and eventually implement the models into a control logic, the output of the models need to be computed online when the ego vehicle is presented with the lead vehicle acceleration. The basic calculation of the driver behavior models is implemented in the subsystem shown in Figure 4.1.

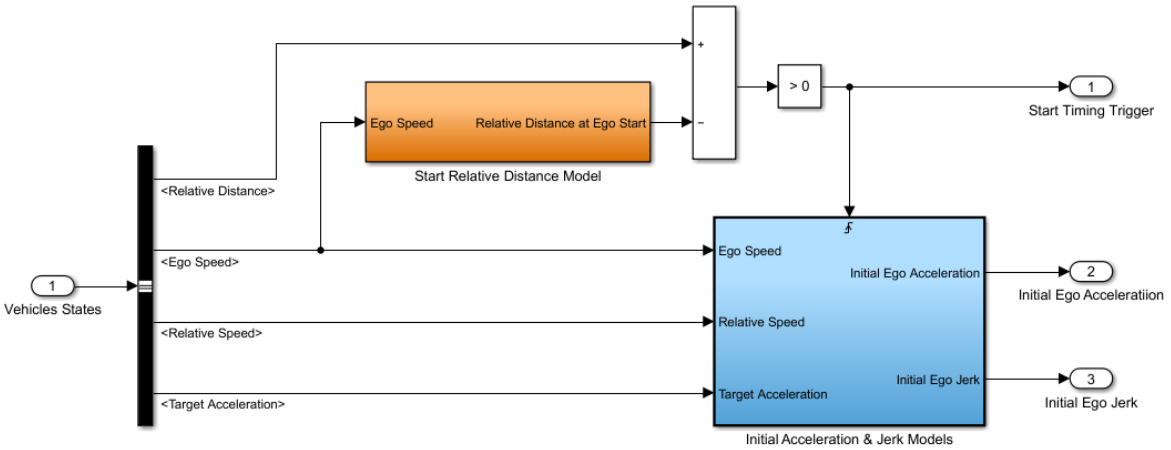

Figure 4.1: Implementation of driver behaviour

The mathematical expressions of the models, already shown in Chapter 3, are implemented in the orange and blue subsystems (Figure 4.1). In order to retain the flexibility given by the type of models fitted, the *aggressiveness* value is set by a parameter in the initialization file of the model. It is important to notice that, while the start relative distance model is computed continuously, the initial acceleration and jerk models are only triggered when the actual relative distance crosses the

threshold set by the start timing model. In the previous chapters the models were fitted with the driving condition (ego speed, relative speed, target acceleration) taken at ego acceleration start timing. This is the reason why the values should not be taken continuously as the conditions would be outside of the fitted range, and the models would provide incorrect values. The output values of the models' subsystem are then processed in order to create the acceleration profile.

The type of output given by the models can be seen by simulating a simple example. Starting from standstill the target vehicle is set to perform a step increase in speed. The simulation results for five different *aggressiveness* levels are shown in Figure 4.2. The results, shown both in terms of speed and acceleration, clearly demonstrate the effect of the *aggressiveness* parameter. By simply varying the *aggressiveness* level, the behaviour of the system is changed to reflect the full range of driving manner. It is worth noting that the axes of Figure 4.2 have been hidden due to confidentiality reasons.

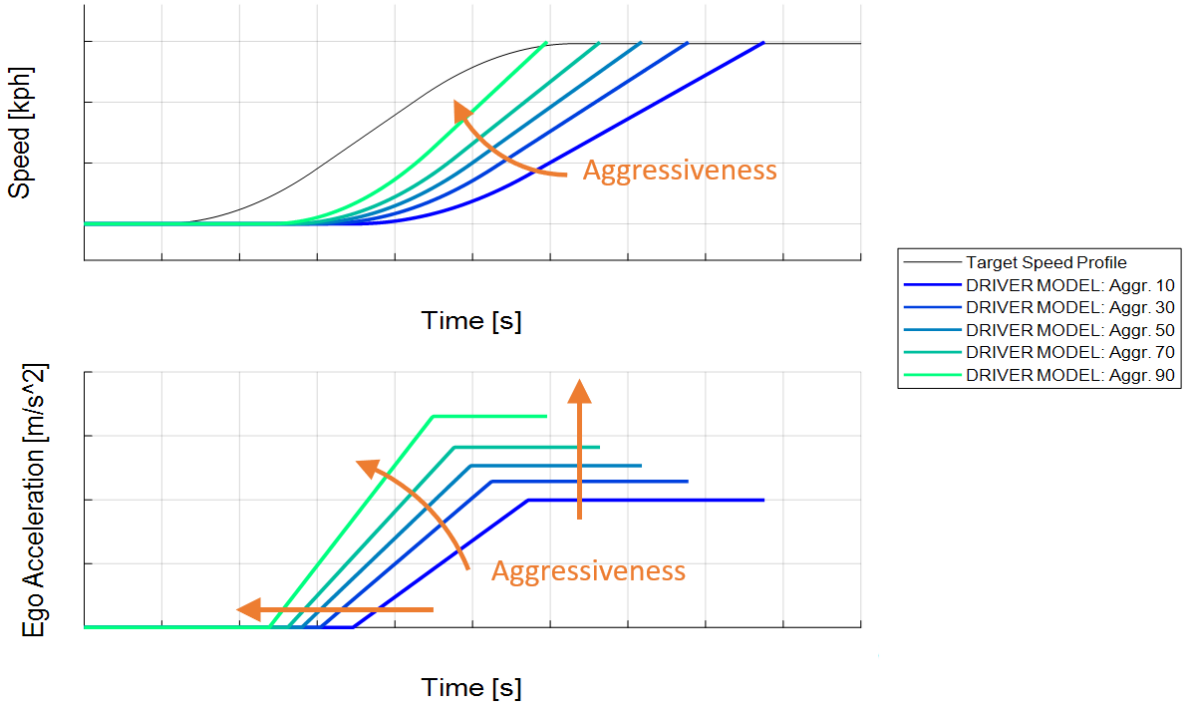

Figure 4.2: Example of implemented models' simulation.

4.2. Comparison with Current ACC Logic

With the implementation of the model explained in the previous section it is possible to perform some comparison simulations. In particular, the initial acceleration reaction starting from a steady following condition. As previously mentioned, the driver behaviour models will be compared to one of current Toyota ACC logic, and numerical values on axes have been hidden for confidentiality reasons. The current system's logic is simulated using SiLS (Software in the Loop Simulation). This means that the exact software loaded in the ECU (Electronic Control Unit) of Toyota vehicles is precompiled and simulated in the Simulink simulation environment.

The target speed profile inputted in the simulation was a step increase with high but realistic acceleration ($> 2 m/s^2$) and a limitation on jerk. The exact values are not disclosed for confidentiality reasons. The simulation was carried out for three different initial driving speeds: 0 km/h, 30 km/h and 70 km/h. Higher speeds were not tested as almost no acceleration scenarios were detected at speeds higher than 80 km/h (see Section 2.4). The ACC system has three different drive mode set-

tings and three distance settings. The results will be shown only for the short distance setting as it does not affect the acceleration and jerk levels of the system. On the other hand, the drive mode directly affects the acceleration levels of the system, for this reason the results will be shown for all three settings: *sport*, *normal* and *eco*.

The first case shown is also the most interesting: initial speed equal to 0 km/h. In Figure 4.3 the simulation results are shown. The main conclusion that can be drawn from the graphs is that current ACC acceleration and jerk levels are significantly lower than the driver behaviour models, even lower than the 10^{th} *aggressiveness* percentile. Looking closer it is possible to see that the jerk level kept by the ACC system is independent of the drive mode, for all three modes the jerk value is lower than the 10^{th} *aggressiveness* percentile. Considering the acceleration, the behaviour of the system slightly differs depending on the drive mode: *sport* mode achieves a higher acceleration level compared to *normal* and *eco* modes which accelerate in a practically identical manner. Nonetheless, for all three modes, the maximum acceleration level is lower than the 10^{th} *aggressiveness* percentile. Using the inverted formulas it is possible to compute what *aggressiveness* level corresponds to the acceleration and jerk values of the system. The *sport* mode acceleration corresponds to the 5.2^{th} *aggressiveness* percentile and the jerk value corresponds to an *aggressiveness* lower than the 5^{th} percentile.

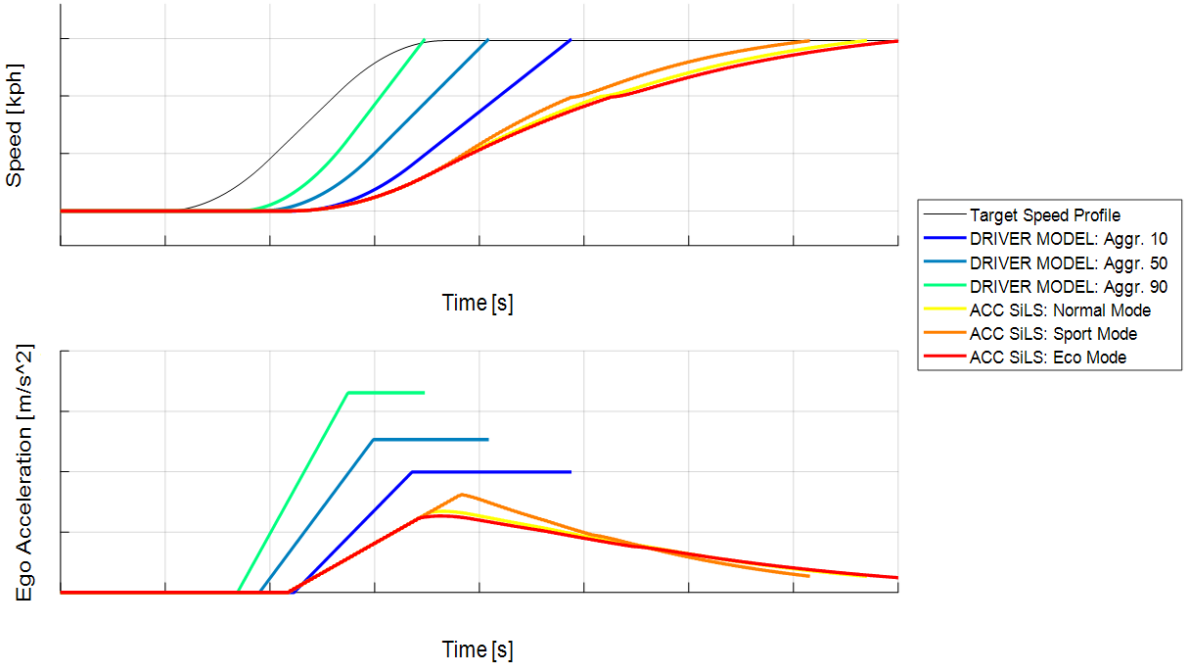

Figure 4.3: Comparison between ACC SiLS and driver behaviour model: 0 km/h initial speed.

This results show that current system, when starting from a standstill position, has a very conservative acceleration level. Most drivers in the same conditions have much higher acceleration and jerk levels. This highlights a potential weak point of the system and if the customer is not satisfied by the behaviour of the system this might lead to annoyance. If the first experiences of the customer with a new system do not match expectations, it is likely that the customer might decide to not use it and simply driving manually.

The remaining two simulated cases are now analyzed. In Figures 4.4 and 4.5 the simulation results are shown for the 30 km/h and the 70 km/h starting speed scenarios respectively. In both cases it is evident that the ACC system is closer to the driver behaviour model compared to the standstill scenario. Now, in both cases, the jerk level of the *normal* drive mode is very close to the one of the 10^{th} *aggressiveness* percentile. Similarly, the acceleration level of the *sport* mode is much closer if

not higher than the one of the 10^{th} *aggressiveness* percentile. That said, the overall behaviour of the system still is considerably more conservative than the driver behaviour, especially when looking at the *eco* drive mode.

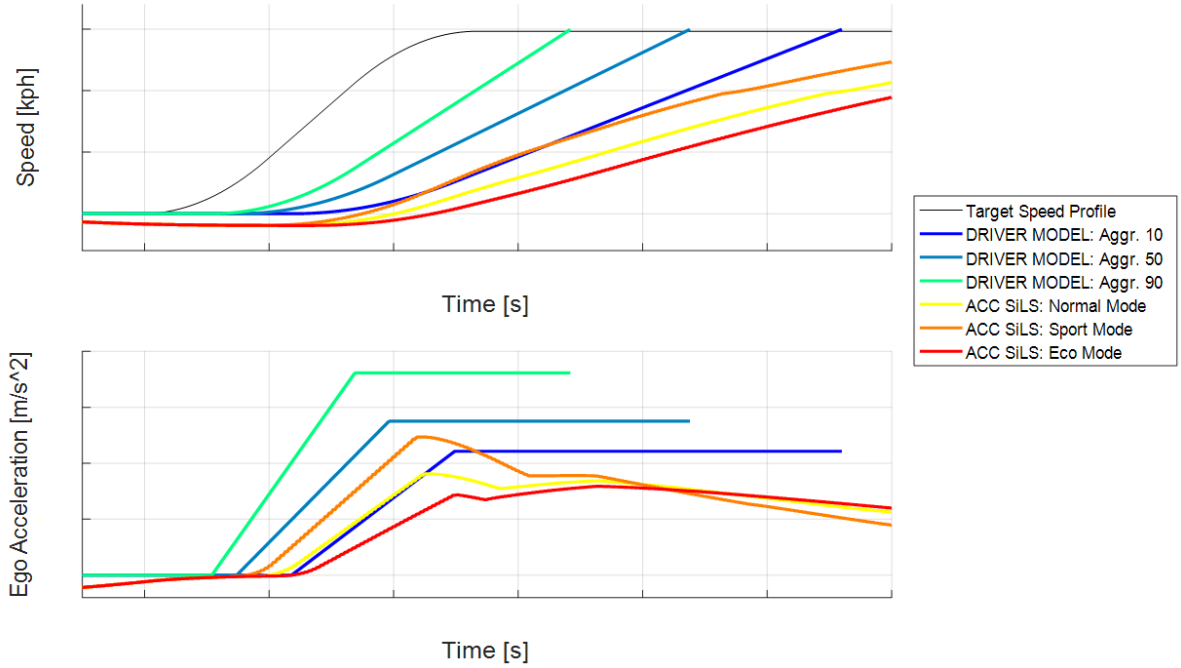

Figure 4.4: Comparison between ACC SiLS and driver behaviour model: 30 km/h initial speed.

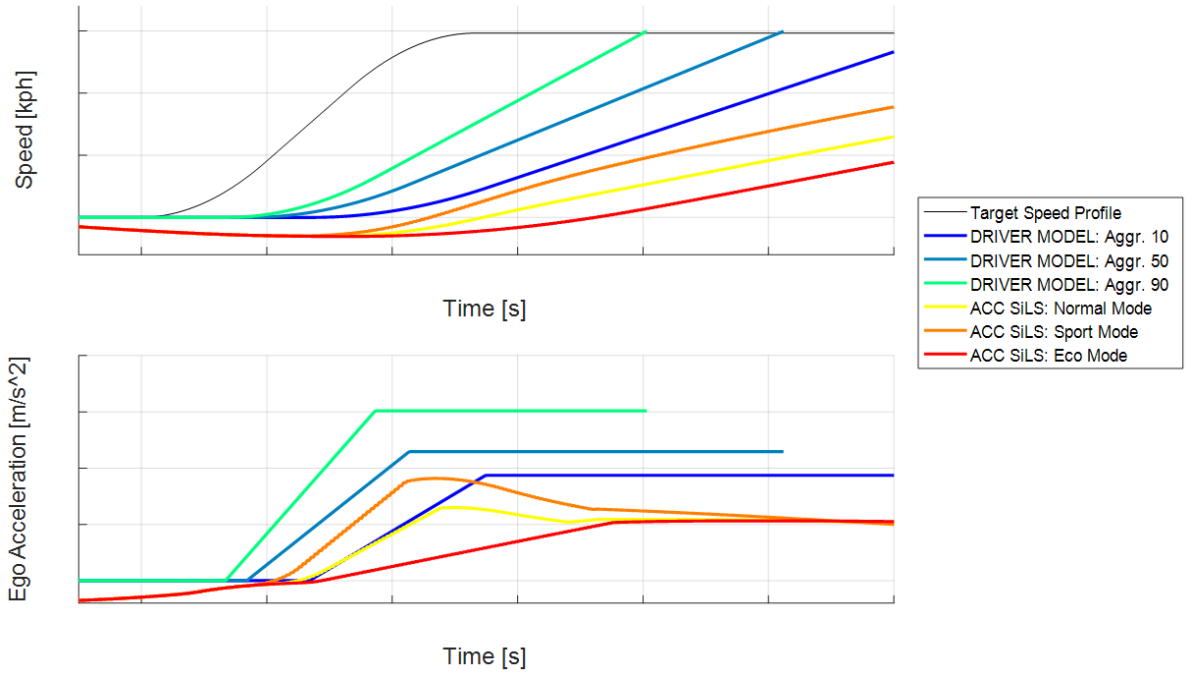

Figure 4.5: Comparison between ACC SiLS and driver behaviour model: 70 km/h initial speed.

As for the standstill scenario, it is possible to compute the equivalent *aggressiveness* value to the the system's behaviour. The results for all drive modes and all simulated starting speeds can be seen in Table 4.1. When looking at the results the first clear conclusion is that the values are quite

low. Clearly the system's behavior is quite far from the average driver behaviour favouring a more conservative acceleration control strategy. This might not be as bothersome to the driver as another clear conclusion from the results: the inconsistency throughout the speed range. Even within the same drive mode the *aggressiveness* value varies significantly at different speed values. This means that the system, depending on the speed condition, will follow a more aggressive or conservative driving style. This might be an unexpected behaviour from the customer point of view which could lead to discomfort.

Table 4.1: Equivalent *aggressiveness* values of ACC SiLS, for each initial speed and drive mode.

	Initial Speed [km/h]		
Drive Mode	**0**	**30**	**70**
Eco	0.4	0.3	0.05
Normal	0.9	5	1
Sport	5.2	35	21

These results, besides from highlighting some potentially small shortcomings of the current system, show the power and flexibility of this methodology. By performing very quick simulations and comparing them with the driver behaviour models it is possible to inspect some specific behaviours of the system without the need to perform tests on real vehicles. This methodology, although not aimed at replacing vehicle validation, can without doubt aid in maximizing the efficiency of the process by saving time and resources.

4.3. String Stability

The driver behaviour implementation includes the start timing model. This model waits until certain conditions are met to initiate the movement of the vehicle, introducing a delay in the control system. This may highlight downsides of the chosen logic when a platoon of vehicles is equipped with this type of system. The delay in the response will amplify the behaviour throughout the platoon creating an undesired performance.

In order to asses the string stability of the driver behaviour models a platoon of six cars is simulated responding to a step increase in speed by the target vehicle. The driver behaviour models are compared to a simplified model of current logic's SiLS, which was technically not possible to simulate in a platoon configuration. In order to carry out the string stability simulation the driver behaviour model implementation, explained previously in Section 4.1, has been enhanced using the Helly car-following model [20]. The modifications to the implementation are explained in Section 4.3.1, while more information about the Helly model can be found in Section 4.3.2.

4.3.1. Implementation for continuous simulation

The models created represent driver behaviour only in a small part of driving conditions: whilst following an accelerating vehicle. Similarly, the model used for the simulations explained in the first part of this chapter is not suitable to simulate any driving condition since it is unable to represent braking and low relative speed conditions. By adding the Helly model alongside the driver behaviour models the new logic can be simulated in every condition. The Helly model was chosen both for its popularity but also for its simplicity. Being linear it can be seen as the simplest approach to ACC design. Practically, the selection between the driver behaviour models and the Helly model is done by using a threshold on the relative speed: if the relative speed is higher than $4\ km/h$, the driver behaviour models are used as a high acceleration from the target vehicle is occurring. For all the other values of relative speed the Helly model logic is selected.

If a simple simulation is performed, similar to the ones done in the beginning of the chapter, it is possible to see when each different logic is in action. In Figure 4.6 is clearly visible when the driver

behaviour models are acting (red line) and when the Helly model takes over (blue line).

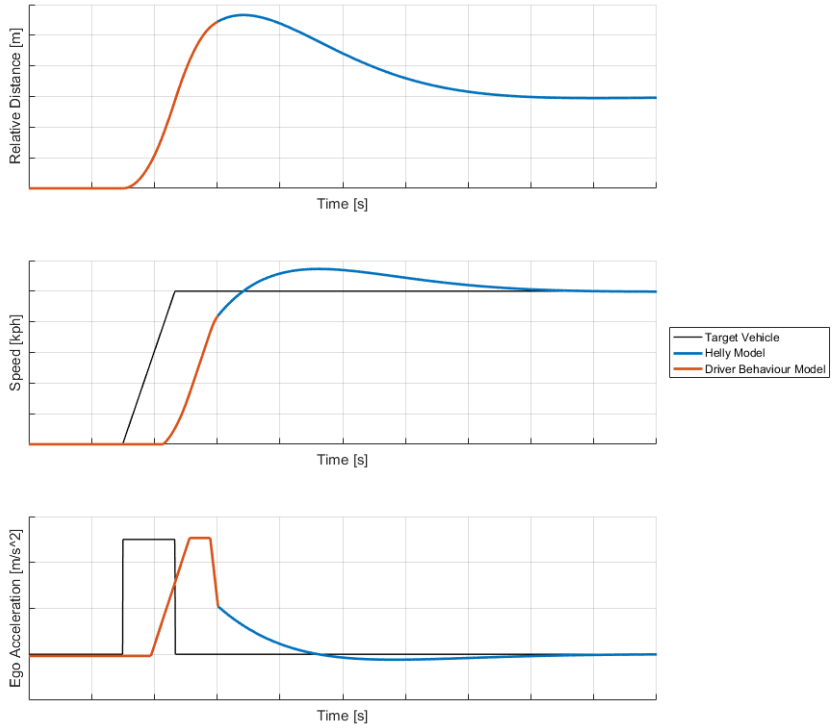

Figure 4.6: Example of the integration of the Helly model with the driver behaviour models.

4.3.2. Helly Linear Model

First introduced by Helly [20] in the late fifties, the Helly model is the most used linear car-following models in literature. The Helly model is typically expressed as:

$$a_e(t) = K_v V_r(t-\tau) + K_d\{D_r(t-\tau) - h_d(t)\} \tag{4.1}$$

$$\text{where} \quad h_d(t) = h_0 + h_v V_e(t) \tag{4.2}$$

The acceleration level is given by two main contributions: the relative speed delayed by a time τ and the difference between the delayed relative distance and the desired following distance h_d. Each of the two contributions are multiplied by a corrective feedback gain, K_v for the relative speed and K_d for the relative distance. The desired following distance is modelled as a linear function of the ego driving speed (V_e), where h_0 represents the desired distance at standstill and h_v the additional THW that describes the dependency of the ego speed.

The interesting feature of the Helly model is that it simplifies the human behaviour to a linear controller, hence the parameters have an intuitive physical meaning. The higher the value of K_v compared to K_d, the bigger the influence of the relative speed in the feedback loop compared to the relative distance will be. Saffarian et al. [41] fitted the Helly model to inspect how the value of the gains changed in different conditions, if the parameters didn't have a physical meaning this procedure would not have been relevant. They also added an extra term to the model: $K_a a_l(t-\tau)$ with a_l being the lead vehicle acceleration and K_a its respective gain. This term models a feedforward contribution to the acceleration control where a unitary gain symbolizes that the driver is willing to follow the lead vehicle's acceleration profile.

4.3.3. Simulation results

Here the results for the string stability comparison are presented. As mentioned earlier, the driver behaviour models logic is compared to a model of current system's logic. String stability will be assessed through the analysis of the simulations results, by measuring the overshoot of the last vehicle of the platoon. The scenario simulated sees the target vehicle performing a step increase starting from standstill. As seen in Section 4.2, this was clearly the most interesting scenario. The target vehicle is followed by six vehicles forming the platoon, each of the following vehicles reacts only to the vehicle immediately in front of it.

The results of the simulation are summarised in Figure 4.7. Most axes are removed for confidentiality apart from the distance and speed axes which are normalized to the final value in order to highlight the overshoot of each logic. As expected, both logics lead to an amplification of the initial input which increases along the platoon length. It is also evident that, in this case, the driver behaviour model is able to perform better than the current logic, keeping the overshoot to a lower value. This performance is reached by achieving a higher acceleration level which is limited in current logic. This was also the key difference of the driver behaviour models highlighted in Section 4.2.

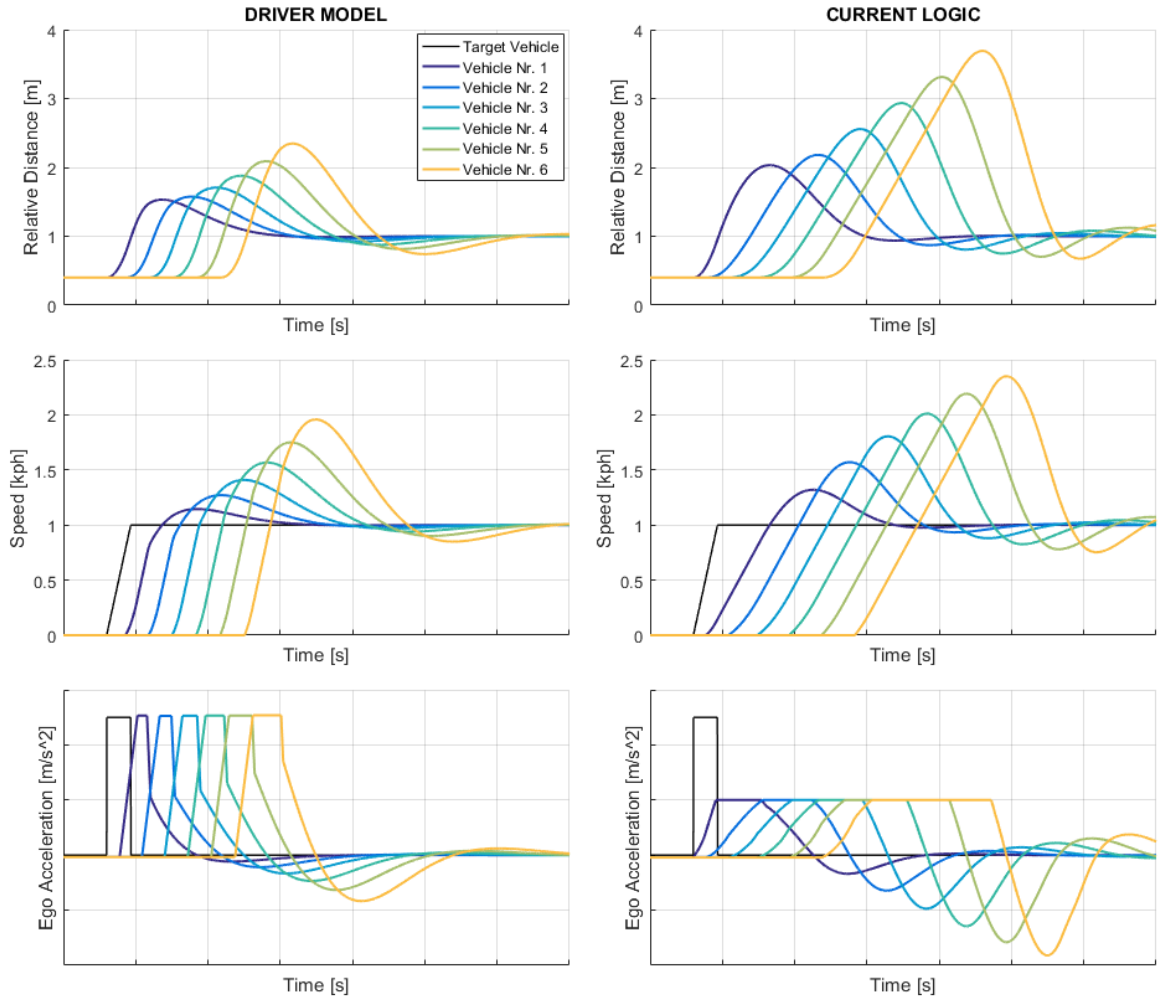

Figure 4.7: Results of string stability simulation.

In order to highlight the differences between the two logics, the first and the sixth vehicles of both results are overlaid in Figure 4.8. The differences between the two logics is even more evident

with this visualization. The simulated maximum overshoot of the sixth vehicle gives a numerical value to the systems performance. In terms of relative distance, the maximum overshoot for the driver models is 2.3, whilst for the current logic this value is 3.7. The overshoots of the speed values give a similar result: 2.0 for the driver behaviour models and 2.4 for current logic. Both looking at relative distance and speed the difference in performance of the two systems is evident. As a comparison, a simulation using only the Helly model is also performed. In Figure 4.8 is possible to see that the Helly model clearly outperforms both logics in terms of string stability. The parameters chosen for the gains are: $K_v = 0.7$ and $K_d = 0.2$, while the delay τ is set to 0. The desired relative distance is set by the start timing driver behaviour model. Is important to notice that the simulated Helly model is still unstable. With the appropriate parameters, this model could be designed to be string stable. The choice of the gains was based on simulating a Helly model with the behaviour of an ACC logic comparable to modern systems. The creation of a string stable logic is beyond the scope of this thesis, the purpose of these simulation is solely to compare the hypothetical behaviour of the analysed logics in the context of a platoon of vehicles.

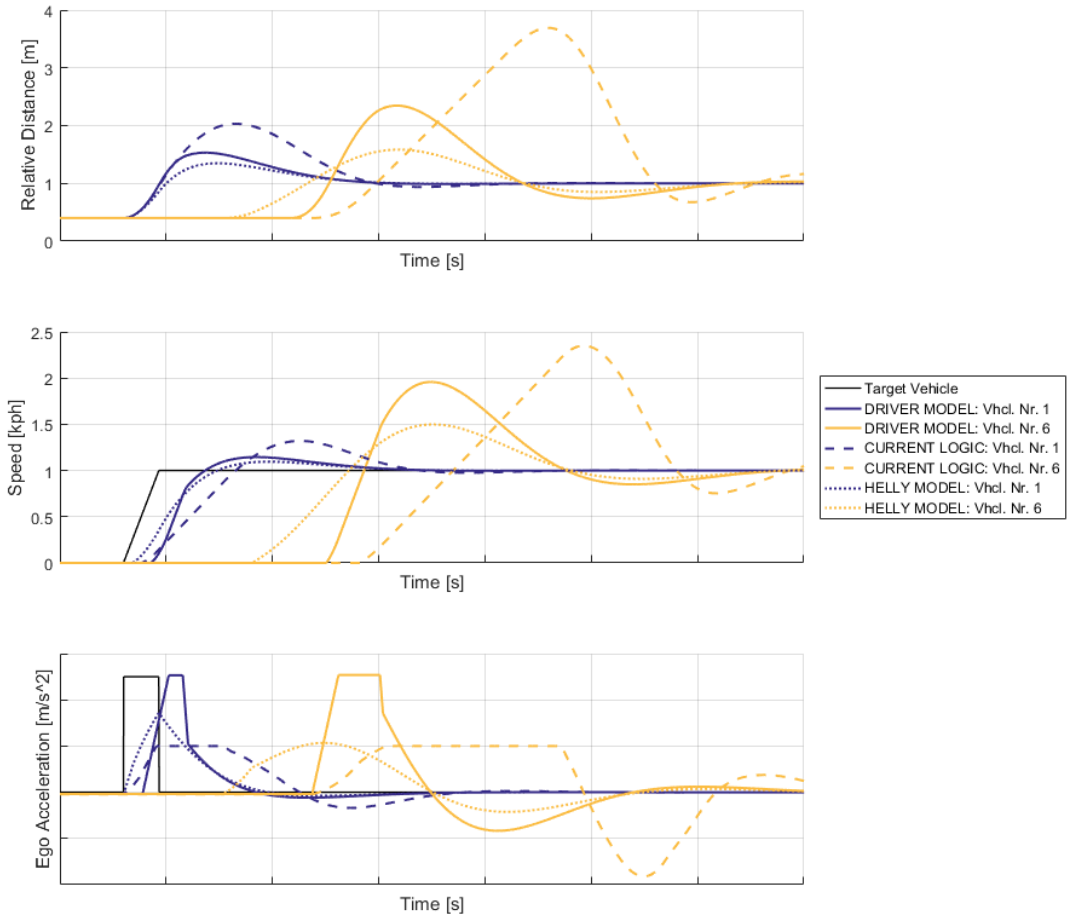

Figure 4.8: String stability results: first and sixth vehicles of both logics and helly model overlaid.

These results show that the higher acceleration response of the driver behaviour models allows them to have an acceptable string stability response especially when compared to the current system model. The delay in the start of reaction given by the start timing model is bridged by the higher acceleration values. Although the performance is acceptable, looking at a not so far future in which every vehicle is equipped with an ACC system, the vehicle capabilities in a platoon scenario should improve. The advent of vehicle to vehicle communication will significantly improve the possibilities of development in these scenarios especially with the help of new technologies like 5G telecommu-

nication. Nonetheless, it is important to highlight that a platoon of vehicles using ACC exists only if the users activate the system, and it is precisely for this reason that the balance between a system able to perform mathematically well and a logic that can be trusted by the user is of crucial importance.

5

Discussion & Conclusion

5.1. Discussion & Recommendations

This section will present the main conclusions of the research, will highlight the novelty of the methodology presented, and will critically assess areas which could be further investigated by future research. The main aim of this project was to answer the following research question and sub questions:

How can Naturalistic Driving Study (NDS) datasets be used in target performance setting for ACC systems?

- *How can the variance of driver behaviour be modelled?*
- *What driving styles are more suitable for the comfort of the driver?*
- *What are the shortcomings of current ACC logic?*
- *How can the logic be improved in accelerating car-following scenarios?*

When performing a study on large datasets the quantity and quality of the data has a major influence on every type of analysis. The French data of the EuroFOT project, one of the largest FOTs in Europe, was used in this project. With a total duration of 13.407 hours, this data contains accurate lead vehicle information (longitudinal and lateral position and velocity) provided by a radar sensor installed in the vehicle. The data was collected and pre-processed by an external supplier, CEESAR partner in the EuroFOT project. Thanks to the experience of the data suppliers, the data provided could be used immediately to start the analysis without the need of any filtering or censoring. The downside of this approach was that direct access to the dataset was not possible as the data was owned by the supplier. This could slow down the debugging process of the detection logic.

The scenario extraction was a preliminary step of the analysis which was just as crucial as the data recording itself: any type of mistake or assumption at this stage could have introduced bias in the analysis. A detection algorithm comprised of many conditions was developed in order to mainly detect two key aspects of the *following an accelerating vehicle* scenario: the acceleration start timing and the initial acceleration level. The former was the most challenging, the algorithm had to find the exact moment in which either the ego or the lead vehicle started accelerating. This was achieved by setting conditions on the average acceleration and jerk of both vehicles, details of the detection logic can be found in Chapter 2. Once the acceleration start timing was found, the initial acceleration level could be extracted. From the whole dataset, a total of 55.096 acceleration episodes were extracted. Alternative detection logics were also taken into consideration. For example, the

use of the throttle input sensor could have been used to give the actual start timing representing the intention of the driver. Unfortunately, the throttle position sensor was often missing and the signal was in general more difficult to post-process due to its quality. In this study the detection algorithm was manually programmed to ensure certain conditions on the extracted scenarios. In the future more advance machine learning methods might be explored such as neural networks or other types of supervised learning algorithms. For the effective use of these type of methods, having free access to the full database will be crucial, which was not the case for this study. The ability to see the video recordings and label the interesting detections is a fundamental step in the performance evaluation of supervised learning algorithms.

The extracted scenarios could finally be used in the analysis in order to create the driver behaviour models. The type of models developed in this study present some differences to what is currently found in literature. The most used models in research like the Helly model [20] or the Intelligent Driver Model (IDM) [22] succeed very well in representing a realistic generic driver behaviour in all conditions. Unfortunately, they are not able to represent different driving styles or precisely represent a particular driving behaviour like hard braking [42]. These are the shortcomings that the models developed in this study are covering. By being based on data percentiles, the models developed can cover the entire variation in driver behaviour in one single parameter incorporated in the model called *aggressiveness*. The variance found in the human behaviour cannot be neglected, if some drivers behaved in a more conservative or aggressive manner it is crucial to understand that in most cases there was a reason for this behaviour which cannot be simplified by simply taking the average behaviour. Moreover, the driver behaviour models developed during this study can also be used to evaluate the *aggressiveness* of a known acceleration episode. This can be quite useful to evaluate the driving style of a specific driver or to assess the performance of existing systems. In this study three models were created to model three crucial aspects of the *following an accelerating vehicle scenario*: initial acceleration level, initial jerk and relative distance at acceleration start. These three models together are capable of modelling the human behaviour in this specific scenario. More details about how the models are created can be found in Chapter 3.

The final step of this study was to implement the models created into a simulation environment. All simulation results can be found in Chapter 4. First the models were compared to a simulation of current ACC logic, secondly the string stability of the model was evaluated. In the first set of simulations the driver behaviour models and the ACC logic were simulated reacting to the same, accelerating, lead vehicle. This was repeated for different starting speed values. The main conclusion from the results was that the current system tends to behave in a quite conservative manner with low acceleration values, especially when starting from standstill. When calculating the *aggressiveness* of the system through the speed range, a second conclusion became apparent. The driving style of the current system not only was quite conservative, but it was also found to change at different starting speeds. This means that the behaviour is not consistent in every condition, an unpredictable behaviour which might surprise the user since the system has different behaviours at different speeds. Since the models were built for specific scenarios, simulating them is challenging, as they cannot be easily used in every driving condition. This was clearly shown in the string stability simulations. In order to carry out the simulation the driver behaviour models' implementation was combined with the Helly model [20]. In this manner the Helly model could take over when the conditions were outside of the operating range of the created models. This new logic created was then compared with a model of current ACC logic by simulating a platoon of six cars following the lead vehicle. As expected, the results showed that both logics were unstable in a string formation. That said, the new logic using the driver behaviour model was clearly less unstable than current ACC. This shows that more natural behaviour can also lead to more stable behaviour. This study on string stability must be seen as a first verification of the logic's performance. It still does not represent the real vehicle performance, and for this reason it is not possible to solely rely on these results. Further checks

need to be done as the logic gets closer to the final product.

The approach explained in this study and finally the expansion of the Helly model showed a potential benefit to fields of research outside of ADAS development, like traffic flow simulation. In his research, Vlaar [22] clearly showed that traditional driver models such as the Helly model and the IDM are not able to mimic the very low acceleration levels reached by human drivers. This type of shortcoming could be solved by extending the models with a driver behaviour model like the ones created in this study. The mentioned models are widely used in the simulation of traffic flow and enhancing them to imitate better human drivers can only benefit the quality of the found results.

The first simulation results showed a clear difference in driving style between the driver behaviour model and current ACC system. The ACC system was clearly more conservative than the human driver, with much lower acceleration values. This difference could be highlighting a mistake in current ACC design or simply answering a very intuitive question: do people want to be driven differently to what they drive? During this study the data used to construct the models was of people driving. However, it is perfectly reasonable to think that, when losing control of the vehicle, the driver will expect the automation to behave more cautiously, especially as he/she builds trust with this new technology. The findings in this research are not enough to answer the question. The assumption is that the correct behaviour is captured in the model, but the desired driving style of the user will be achieved by selecting the correct value of *aggressiveness*. This must be done with further validation, possibly in a driving simulator or in a prototype vehicle. In this way it will be possible to check if people tend to decrease their preferred *aggressiveness* value when they lose control of the vehicle.

The modelling approach followed in this paper could also be extended to other driving scenes beyond *following an accelerating vehicle*. Some interesting scenes could be for example: *steady following* and *braking*. Every scene can be modelled as long as the three key components of the model can be identified: driving scene, driving behaviour and driving manner (Figure 1.1). Once the main scenes are studied it would also be interesting to see how they interact. For example, in Section 1.3.1 it was explained how the *steady following* scenario is tied to the *following an accelerating vehicle* scenario. Further research could answer questions like: in which conditions does the transition between these scenarios happen? Can this behaviour be modelled? Once these important questions are answered it is crucial to check if the models created in this study are still valid or if they need some modifications.

5.2. Conclusion

This master thesis project showed how driver behaviour models built using driving data can be used to improve the target performance of future ACC systems. Data driven methods for the development of ADAS and AD systems are inevitably going to increase in importance. Not only for the training of recognition algorithms but also in the development of control logics. The potential of the information that resides in the data can be very rich despite sometimes being challenging to extract. This study covered the modelling of drivers in “normal” driving conditions, similar approaches could be used in studying the limit cases or the safety critical situations by looking at the extreme data percentiles. AD systems must be ready to cope with every situation they are presented with. Even the least occurring ones.

The process explained in this thesis, together with the validation and implementation of the models, has to be seen as cyclic. In each iteration the models highlight the critical point of the current implementation whilst the implementation highlights what is still missing in the models. With regards to the latter, this refers to the cases in which the analysis approximates too much the human behaviour and is therefore in need of being expanded. Even if some ADAS like ACC have been on the market for many years, it is only recently that these technologies are becoming widespread and that customers are starting to get accustomed to them. By using driver behaviour models this process is

facilitated as the behaviour of the vehicle is familiar and predictable, the controller becomes part of the Human Machine Interface (HMI). As the customer gets more familiar with this technology his expectation will also increase and change, especially as the levels of automation start to increase. This will inevitably push automakers to continue to improve the technology to deliver increasingly advanced and safe vehicles, in the hope that one day the ultimate industry target of zero accidents will be achieved.

Bibliography

[1] S. O.-R. A. V. S. Committee *et al.*, *Taxonomy and definitions for terms related to on-road motor vehicle automated driving systems,* SAE Standard J3016 , 01 (2014).

[2] T. Gordon and M. Lidberg, *Automated driving and autonomous functions on road vehicles,* Vehicle System Dynamics **53**, 958 (2015).

[3] Lexus, *2018 lexus ls packages,* Retrieved 2018-01-22, https://www.lexus.com/models/2018LS/packages .

[4] V. Nguyen, *Meet the new 2019 audi a8 a self-driving super-luxury sedan,* Retrieved 2018-01-22 from https://www.slashgear.com/meet-the-new-2019-audi-a8-a-self-driving-super-luxury-sedan-11491106/ .

[5] A. LaFrance, *Self-driving cars could save 300,000 lives per decade in america,* Retrieved 2018-01-22 from https://www.theatlantic.com/technology/archive/2015/09/self-driving-cars-could-save-300000-lives-per-decade-in-america/407956/ .

[6] B. Crew, *Driverless cars could reduce traffic fatalities by up to 90%, says report,* Retrieved 2018-01-22 from https://www.sciencealert.com/driverless-cars-could-reduce-traffic-fatalities-by-up-to-90-says-report .

[7] EuroFOT, *Eurofot: Bringing intelligent vehicles to the road.* .

[8] P. Bansal and K. M. Kockelman, *Forecasting americans' long-term adoption of connected and autonomous vehicle technologies,* Transportation Research Part A: Policy and Practice **95**, 49 (2017).

[9] B. M. Muir, *Trust in automation: Part i. theoretical issues in the study of trust and human intervention in automated systems,* Ergonomics **37**, 1905 (1994).

[10] J. M. Flach, *Control with an eye for perception: Precursors to an active psychophysics,* Ecological Psychology **2**, 83 (1990).

[11] J. Gibson, *Percept vis world,* Houghton Mifflin, Boston (1950).

[12] J. J. Koenderink, *Optic flow,* Vision research **26**, 161 (1986).

[13] C. J. Nash, D. J. Cole, and R. S. Bigler, *A review of human sensory dynamics for application to models of driver steering and speed control,* Biological cybernetics **110**, 91 (2016).

[14] D. A. Gordon, *Static and dynamic visual fields in human space perception,* Josa **55**, 1296 (1965).

[15] G. L. Zacharias, A. K. Caglayan, and J. B. Sinacori, *A model for visual flow-field cueing and self-motion estimation,* IEEE Transactions on Systems, Man, and Cybernetics , 385 (1985).

[16] M. Taieb-Maimon and D. Shinar, *Minimum and comfortable driving headways: Reality versus perception,* Human factors **43**, 159 (2001).

[17] W. Van Winsum, *The human element in car following models,* Transportation research part F: traffic psychology and behaviour **2**, 207 (1999).

[18] W. V. WINSUM and A. Heino, *Choice of time-headway in car-following and the role of time-to-collision information in braking,* Ergonomics **39**, 579 (1996).

[19] M. Brackstone and M. McDonald, *Car-following: a historical review,* Transportation Research Part F: Traffic Psychology and Behaviour **2**, 181 (1999).

[20] W. Helly, *Simulation of bottlenecks in single-lane traffic flow,* (1959).

[21] D. C. Gazis, R. Herman, and R. W. Rothery, *Nonlinear follow-the-leader models of traffic flow,* Operations research **9**, 545 (1961).

[22] M. Treiber, A. Hennecke, and D. Helbing, *Congested traffic states in empirical observations and microscopic simulations,* Physical review E **62**, 1805 (2000).

[23] R. Michaels, *Perceptual factors in car following,* in *Proceedings of the 2nd International Symposium on the Theory of Road Traffic Flow (London, England), OECD* (1963).

[24] J. J. Lee and J. Jones, *Traffic dynamics: visual angle car following models,* Traffic Engineering & Control **8** (1967).

[25] L. Evans and R. Rothery, *Experimental measurements of perceptual thresholds in car-following,* 464 (1973).

[26] P. Fancher and Z. Bareket, *Evolving model for studying driver-vehicle system performance in longitudinal control of headway,* Transportation Research Record: Journal of the Transportation Research Board , 13 (1998).

[27] N. Van Nes, M. Houtenbos, and I. Van Schagen, *Improving speed behaviour: the potential of in-car speed assistance and speed limit credibility,* IET Intelligent Transport Systems **2**, 323 (2008).

[28] S. Schleicher, C. Gelau, *et al.*, *The influence of cruise control and adaptive cruise control on driving behaviour–a driving simulator study,* Accident Analysis & Prevention **43**, 1134 (2011).

[29] C. M. Rudin-Brown and H. A. Parker, *Behavioural adaptation to adaptive cruise control (acc): implications for preventive strategies,* Transportation Research Part F: Traffic Psychology and Behaviour **7**, 59 (2004).

[30] B. D. Seppelt and J. D. Lee, *Making adaptive cruise control (acc) limits visible,* International journal of human-computer studies **65**, 192 (2007).

[31] C. Diels and J. E. Bos, *Self-driving carsickness,* Applied ergonomics **53**, 374 (2016).

[32] A. Rolnick and R. Lubow, *Why is the driver rarely motion sick? the role of controllability in motion sickness,* Ergonomics **34**, 867 (1991).

[33] P. Feenstra, J. E. Bos, and R. N. van Gent, *A visual display enhancing comfort by counteracting airsickness,* Displays **32**, 194 (2011).

[34] A. M. Bronstein, J. F. Golding, and M. A. Gresty, *Vertigo and dizziness from environmental motion: visual vertigo, motion sickness, and drivers' disorientation,* in *Seminars in neurology*, Vol. 33 (Thieme Medical Publishers, 2013) pp. 219–230.

[35] T. Helldin, G. Falkman, M. Riveiro, and S. Davidsson, *Presenting system uncertainty in automotive uis for supporting trust calibration in autonomous driving,* in *Proceedings of the 5th International Conference on Automotive User Interfaces and Interactive Vehicular Applications* (ACM, 2013) pp. 210–217.

[36] J. Koo, J. Kwac, W. Ju, M. Steinert, L. Leifer, and C. Nass, *Why did my car just do that? explaining semi-autonomous driving actions to improve driver understanding, trust, and performance,* International Journal on Interactive Design and Manufacturing (IJIDeM) **9**, 269 (2015).

[37] A. Waytz, J. Heafner, and N. Epley, *The mind in the machine: Anthropomorphism increases trust in an autonomous vehicle,* Journal of Experimental Social Psychology **52**, 113 (2014).

[38] S. Moon and K. Yi, *Human driving data-based design of a vehicle adaptive cruise control algorithm,* Vehicle System Dynamics **46**, 661 (2008).

[39] FOT-net, *Eurofot: Bringing intelligent vehicles to the road.* .

[40] B. Sultan, M. Brackstone, and M. McDonald, *Drivers' use of deceleration and acceleration information in car-following process,* Transportation Research Record: Journal of the Transportation Research Board , 31 (2004).

[41] M. Saffarian, J. C. De Winter, and R. Happee, *Enhancing driver car-following performance with a distance and acceleration display,* IEEE Transactions on Human-Machine Systems **43**, 8 (2013).

[42] T. Vlaar, *Car following model of the distracted driver,* (2015).